Cancer research (New drugs)

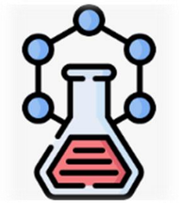

Synthetic compound

Natural products

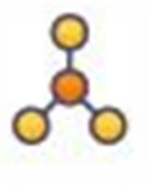

Pure compound ← Extracted product

Drug → Chemotherapy

Supplementary food → Chemoprevention

Advantage

Experiments

http://blogs.discovermagazine.com

In vitro (Cell culture)

https://labcat.com/in-life-in-vivo/

In vivo

- Animal ethics
- Human ethics

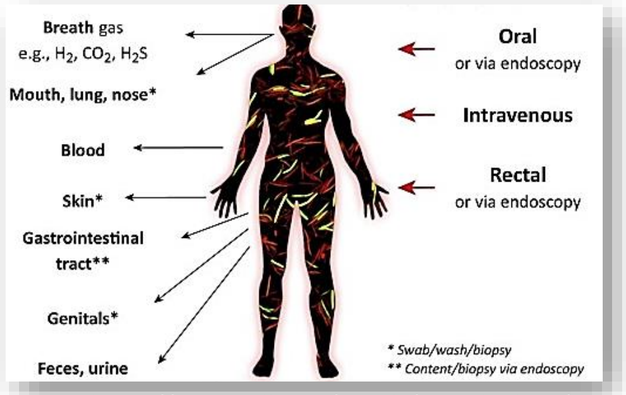

https://www.cell.com/trends/microbiology/fulltext/S0966-842X(18)30139-2

In silico (Program computer)

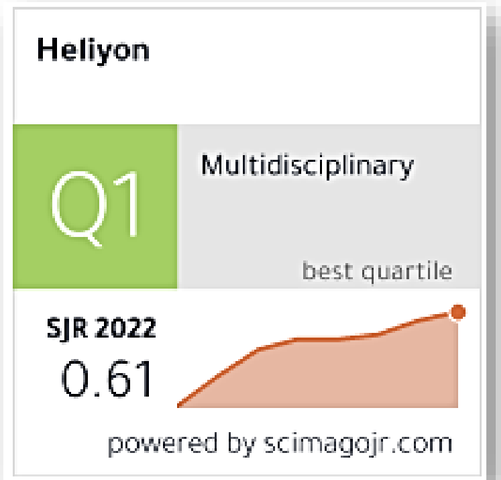

What is Heliyon impact factor 2023?

The 2022-2023 Journal's Impact IF of Heliyon is 3.776, which is just updated in 2023.

Academic Accelerator
https://academic-accelerator.com › Impact-of-Journal

Heliyon Latest Journal's Impact IF - Trend · Prediction · Ranking

Heliyon 7 (2021) e07749

Contents lists available at ScienceDirect

Heliyon

journal homepage: www.cell.com/heliyon

Research article

Anticancer activity of RAPTA-EA1 in triple-negative BRCA1 proficient breast cancer cells: single and combined treatment with the PARP inhibitor olaparib

Khwanjira Hongthong [a], Tidarat Nhukeaw [a], Pornvichai Temboot [a], Paul J. Dyson [b], Adisorn Ratanaphan [a,*]

[a] Laboratory of Pharmaceutical Biotechnology, Department of Pharmaceutical Chemistry, Faculty of Pharmaceutical Sciences, Prince of Songkla University, Hat-Yai, Songkhla 90112, Thailand
[b] Institute of Chemical Sciences, and Engineering, Swiss Federal Institute of Technology Lausanne (EPFL), CH-1015 Lausanne, Switzerland

ARTICLE INFO

Keywords:
Anti-cancer drugs
Metal-based drugs
BRCA1
RAPTA-EA1
Olaparib

ABSTRACT

RAPTA-EA1 is a promising glutathione transferase (GSTP-1) inhibitor that has previously been shown to inhibit the growth of various breast cancer cells. We studied the anticancer activity of RAPTA-EA1 on triple-negative BRCA1 competent breast cancer MDA-MB-231 cells. MDA-MB-231 cells are significantly more sensitive to RAPTA-EA1 than MCF-7 cells. Treatment reveals a higher degree of cytotoxicity than cisplatin against both cell lines. Ruthenium accumulation in MDA-MB-231 cells is mainly in the nuclear fraction (43%), followed by the cytoplasm (30%), and the mitochondria (27%). RAPTA-EA1 blocks cell growth at the G2/M phase, leading to nuclear condensation and cell death. The compound slightly inhibits DNA replication of the 3,426-bp fragment of the BRCA1 exon 11 of the cells, with approximately 0.6 lesion per the BRCA1 fragment. The expression of BRCA1 mRNA and its protein in the Ru-treated cells is curtailed by 50–80% compared to the untreated controls. Growth inhibition of the triple-negative BRCA1 wild-type MDA-MB-231 and the sporadic BRCA1 wild-type MCF-7 cells by olaparib (a poly [ADP-ribose] polymerase (PARP) inhibitor) is dose-dependent, with MDA-MB-231 cells being two-fold less susceptible to the drug than MCF-7 cells. Combining olaparib with RAPTA-EA1 results in a combination index (CI) of 0.78 (almost additive) in MDA-MB-231 cells and 0.24 (potent synergy) in the MCF-7 cells. The PARP inhibitor alone differently regulates the expression of BRCA1 mRNA in both cell lines, whereas the olaparib-RAPTA-EA1 combination induces overexpression of BRCA1 mRNA in these cells. However, the expression level of the BRCA1 protein is dramatically reduced after treatment with the combined inhibitors, compared with the untreated controls. This observation highlights the cellular responses of triple-negative BRCA1 proficient breast cancer MDA-MB-231 cells to RAPTA-EA1 through BRCA1 inhibition and provides insights into alternative treatments for breast cancer.

1. Introduction

Breast cancer is a diverse disease and has been classified into biological subtypes with distinct histopathological, genetic and epigenetic characteristics [1]. Based on gene expression profiling, breast cancer can be divided into five major breast tumor subtypes that include, luminal A, luminal B, overexpression of human epidermal growth factor receptor 2 (HER2), basal-like, and normal breast-like. The basal-like subtypes have distinctive histological features, response to chemotherapy, and clinical outcomes. Patients with basal-like cancers have main characteristics similar to those with the triple-negative breast cancers (TNBC) that are defined as none expression of estrogen receptor (ER), progesterone receptor (PR), and HER2, which are often observed in younger patients (<50 years) and more frequently in African-American women and black ethnicities [1]. TNBC patients exhibit important clinical implications with diverse histology, high grade, and high rate of recurrence and metastases within 5 years of the initial diagnosis. They have a poorer overall survival than other subtypes of breast cancers and do not normally benefit from currently viable targeted therapies, such as endocrine or anti-HER2 agents, and consequently, these patients rely primarily on only systemic treatment options, and chemotherapy with standard cytotoxic agents [2]. Currently, there is no preferred standard form of chemotherapy for TNBC. The first-line treatment for TNBC includes a combination of surgery, radiation, and neoadjuvant/adjuvant chemotherapy. In a clinical study, TNBC patients who received platinum-based drugs had a significantly higher pathological response compared to patients treated with non-platinum drugs (64.3 versus 49.2%) [2]. However, platinum-based drugs have several disadvantages such as induced secondary mutations, acquired resistance and high general toxicity [3]. Many non-platinum-based metal complexes have therefore been investigated as new leads that potentially overcome the limitations of platinum compounds. One promising class is ruthenium-based complexes, including arene-ruthenium (II)-complexes containing PTA (1,3,5-triaza-7-phosphaadamantane), often termed RAPTA (Figure 1) [4].

RAPTA compounds such as RAPTA-C and RAPTA-T exhibit antimetastatic [5] and antiangiogenic [6] properties and are active against various tumor types [7, 8]. It appears that while these compounds can bind to DNA, they preferentially bind to proteins [9, 10]. It has been reported that RAPTA compounds perturb the BRCA1 RING protein domain secondary structure, resulting in the displacement of zinc ions, and leading to loss of BRCA1-mediated E3 ubiquitin ligase activity [11]. A RAPTA compound with ethacrynic acid (EA) tethered to the arene ring, termed RAPTA-EA1, is a strong inhibitor of glutathione-S-transferase P1 (GSTP-1) that inhibits growth of various cancer cells [5, 12]. GSTP-1 represents the most prevalent mammalian isoenzyme of glutathione S-transferases (GSTs) that plays an important role in detoxification and antioxidant defense [12]. It has recently been shown that GSTP-1 inhibition is a promising strategy for TNBC treatment [13]. Previous studies have shown that ruthenium (II)-based compounds exhibited promising anticancer activities to treat BRCA1-defective TNBC [14, 15, 16, 17]. The BRCA1 gene responds to DNA damage through multi-cellular pathways including cell cycle regulation, ubiquitination, DNA repair and transcription [14, 15, 16, 17]. RAPTA-EA1 exhibits different cellular responses for the triple-negative BRCA1-mutant HCC1937 cells and the sporadic BRCA1-wild type MCF-7 cells [18]. Differences in anticancer activity were associated with differential ruthenium uptake into breast cancer cells and subsequent apoptosis. RAPTA-EA1 induced significantly more damage to the BRCA1 gene in the BRCA1-mutant HCC1937 cells than to the BRCA1-wild type MCF-7 cells, and reduced the expression level of the BRCA1 protein in both types of breast cancer cells as well [18].

A combination treatment comprising cisplatin and a PARP inhibitor is one of the therapeutic options used to improve the treatment of BRCA1-deficient breast cancer cells [19]. One of the potential PARP inhibitors is olaparib, enhancing synthetic lethality in BRCA1-deficient cancer cells [20], i.e. the cancer cells harboring the mutated BRCA1 gene are

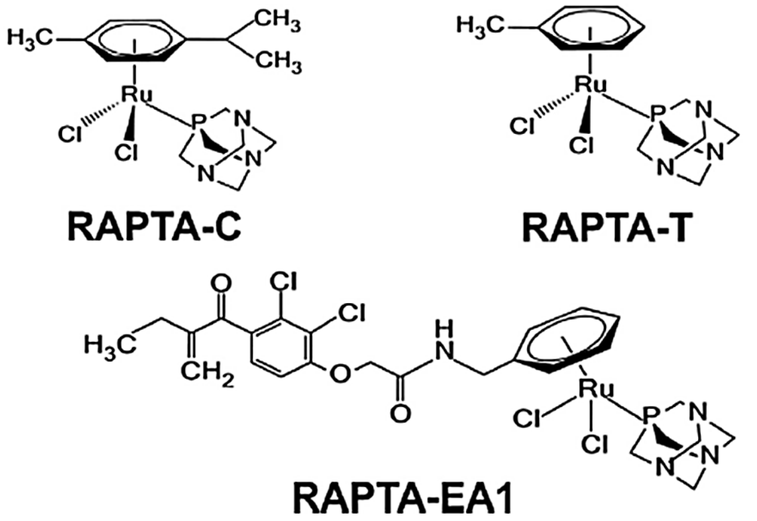

Figure 1. Chemical structure of the arene-ruthenium (II)-complexes containing PTA (1,3,5-triaza-7-phosphaadamantane, often termed RAPTA.

defective in homologous recombination repair [21]. Recent clinical trials assessing olaparib in combination with platinum-based drugs reveal encouraging efficacies [22, 23]. Using olaparib in combination with other metal-based drugs, i.e., cisplatin or carboplatin has been studied in pre-clinical models as a new targeted therapy against BRCA-deficient cancers [22, 23].

The MDA-MB-231 cell line, isolated at MD Anderson from a pleural effusion of a patient with invasive ductal carcinoma, is commonly used to model late-stage breast cancer, and are a good model of TNBC. TNBC MDA-MB-231 cells are resistant to many anti-cancer agents [24, 25, 26], although they are sensitive to some ruthenium (II)-arene complexes [24, 25, 26]. To address the effect of RAPTA-EA1 on this particular subtype of breast cancer cells, hence, we decided to evaluate the anticancer efficacy of RAPTA-EA1 against triple-negative BRCA1 wild-type breast cancer MDA-MB-231 cells through BRCA1 inhibition. Combination treatment of the PARP inhibitor olaparib with RAPTA-EA1 is also reported, in comparison with the sporadic BRCA1 wild-type MCF-7 cells.

Objectives

* Corresponding author.
E-mail address: adisorn.r@psu.ac.th (A. Ratanaphan).

https://doi.org/10.1016/j.heliyon.2021.e07749
Received 24 February 2021; Received in revised form 8 June 2021; Accepted 6 August 2021

2. Materials and methods

2.1. Materials

RAPTA-EA1 was prepared using a literature method [18]. Cisplatin was obtained from Sigma-Aldrich (USA), and prepared as stock solutions (1–5 mM) in deionized water.

2.2. Cell culture

Human breast cancer cell lines, triple-negative MDA-MB-231 (BRCA1 wild-type) and MCF-7 (sporadic BRCA1 wild-type), were procured from the American Type Culture Collections (ATCC, Rockville, MD). Cells were seeded in 6-well plates with 1 mL of Dulbecco's modified eagle's medium (DMEM) without phenol red, supplemented with fetal bovine serum 10% (FBS), penicillin-streptomycin 1%. Cells were incubated in 5% CO_2 at 37 °C.

2.3. MTT proliferation assay

About 5×10^4 cells (MDA-MB-231 or MCF-7) were plated into each well of a 96-well culture plate and incubated for 48 h at 37 °C in a 5% CO_2 incubator. The culture medium was then removed and 200 µL of fresh culture medium with various concentrations of RAPTA-EA1 and cisplatin (as a control) was added. The breast cancer cells were further incubated for 48 h. After incubation, each well of the 96-well culture plate was then washed twice with 100 µL of phosphate-buffered saline (PBS). The solution of 3-(4,5-dimethylthiazol-2-yl)-2,5-diphenyl tetrazolium bromide (MTT) (0.5 mg/mL) was added to each well and incubated for additional 4 h. The MTT solution was gently removed and dimethylsulfoxide (200 µL) was added to solubilize the crystals of purple fomazan formed. The absorbance of each well was spectrophotometrically measured at 570 nm using an automated microplate reader. The cell viability (%) was calculated as follows:

$$\textit{Cell viability}\ (\%) = (\textit{absorbance of the Ru} - \textit{treated cells} / \textit{absorbance of the control}\ (\textit{Ru} - \textit{untreated cells}))\ x\ 100$$

Percentage cell viability was plotted against various concentrations of the ruthenium compound or cisplatin to determine the 50% inhibitory concentration (IC_{50}), defined as the concentration of the ruthenium compound or cisplatin which inhibited cell viability by at least 50% compared to the control condition [18].

2.4. Cellular accumulation and distribution

About 5×10^6 MDA-MB-231 cells were incubated with RAPTA-EA1 (IC_{50} concentration of 10 µM, Table 1) at 37 °C for 48 h under 5% CO_2 [18]. Cells were washed twice with 5 mL of PBS buffer and the cells were then fractionated, and the ruthenium content distributed in the cytoplasm, mitochondria and nucleus was determined by means of mass spectrometry equipped with inductively coupled plasma (ICP-MS) (Agilent Technologies, USA) [27].

2.5. Cell cycle analysis

Approximately 10^6 MDA-MB-231 cells were added into 6-well culture plates and grown at approximately 80% confluence. The cells were treated with RAPTA-EA1 (IC_{50} concentration of 10 µM) or cisplatin (128 µM) (Table 1) at 37 °C for 48 h under 5% CO_2. The breast cancer cells were then prepared as described previously [14]. Briefly, cells were trypsinized using 0.25% trypsin, washed with PBS buffer, and then centrifuged at 300 g for 5 min. The cells were collected and fixed with cold ethanol (70%) and stored overnight at 20 °C. The cell pellets were washed and re-suspended in PBS (1 mL) containing RNase (100 µg/mL), PI (50 µg/mL), and Triton-X-100 (0.1%), and then placed in an incubator at 37 °C for 30 min in the dark. Fluorescence was recorded using a FACSCanto flow cytometer. MultiCycle software was used to analyze the cell cycle distribution, which represents the percentages of the cells at the G0/G1, S and G2/M phases.

2.6. Apoptosis detection by Annexin V

Approximately 10^6 MDA-MB-231 cells were added into 6-well plates and grown to approximately 80% confluent. The cells were treated with RAPTA-EA1 (IC_{50} concentration of 10 µM) or cisplatin (128 µM) (Table 1) at 37 °C for 48 h under 5% CO_2. After incubation, the cells were harvested, washed twice with PBS buffer, and then centrifuged at 300g for 5 min. One hundred microliter of 1x Annexin-binding buffer was filled to re-suspend the cell pellets. Alexa-Fluor 488 Annexin-V (5 µL), and PI (1 µL) (at 100 µg/mL) were added and the cells were further incubated at room temperature for 15 min. The solution of 1x Annexin-binding buffer (400 µL) was subsequently added. Analysis of Annexin-V binding was performed using a FACSCanto flow cytometer with an excitation wavelength of 488 nm [8, 18].

2.7. Immunofluorescence assay

MDA-MB-231 cells treated with RAPTA-EA1 (10 µM) were incubated at 37 °C for 48 h were seeded on coverslips, fixed with 4% paraformaldehyde for 30 min, and then permeabilized with 0.2% Triton X-100. The cells were incubated with blocking reagent [(3% bovine serum albumin in Tris buffered saline with 0.1% Tween x20 (TBST)] for 1 h at room temperature and then their nuclei were counterstained with 4′, 6-diamidio-2-phenylindole (DAPI; 1 µg/mL).

2.8. Utilization of QPCR for cellular BRCA1 damage

RAPTA-EA1 at a various concentration (0–100 µM) was incubated with MDA-MB-231 cells at 37 °C for 48 h under CO_2 5%. The genomic DNA of MDA-MB-231 cells was collected as previously described [18]. The BRCA1 fragment (exon 11, 3426 bp) was used as the DNA target and then amplified by PCR [14]. The reaction mixture (50 µL) consisted of a ruthenated genomic-DNA template at 400 ng, the forward primer (5′-GCCAGTTGGTTGATTTCCACC-3′) and reverse primer (5′-GTAAAATGTGCTCCCCAAAAGC-3′) was kept as 0.5 µM, $MgCl_2$ (300 µM) 1xPhusion™ GC Buffer, and Phusion Hot-Start DNA-polymerase 2 units. Amplification of BRCA1 was performed using PCR following initial denaturation at 94 °C for 3 min; 30 cycles of 30 s at 94 °C, 45 s at 60 °C, 2 min at 72 °C, and a final extention for 7 min at 72 °C. PCR products were electrophoresed on 1% agarose gels at 100 V. Gel staining was done with ethidium bromide and imaged in the presence of ultraviolet light. The band intensity indicated the magnification of products quantified on a Bio-Rad Molecular Imager Densitometer along with the Molecular Dynamics program (version 1.0.2. Bio-Rad, Hercules, CA, USA, 1994). The amount of DNA amplification (%) was plotted as a function of concentration. RAPTA-EA1-induced BRCA1 fragment (lesions per the 3426-bp fragment) in MDA-MB-231 cells was calculated using the Poisson equation [14]. Experiments were conducted in triplicate.

2.9. Quantitative analysis of expression of BRCA1 mRNA following RAPTA-EA1 treatment using real-time quantitative RT-PCR

MDA-MB-231 cells treated with RAPTA-EA1 (10 μM) were incubated at 37 °C for 48 h. The cells were harvested, and the total cellular RNA was isolated using an RNeasy® Mini Kit (Qiagen, Germany) according to the manufacturer's protocol. Total RNA (1 μg) was used for the first strand synthesis of complimentary-DNA through QuantiTech® Reverse-Transcription (Qiagen, Germany) following the manufacturer's instructions. Specific primers for DNA amplification; BRCA1 forward: 5′-GCCAGTTGGTTGATTTCCACC-3′; BRCA1 reverse: 5′-GTCAAATGTGCTC CCCAAAAGC-3′; β-Actin forward: 5′-CCGTAAAGACCTCTATGCCAACA-3′; β-Actin reverse: 5′-CGGACTCATCGTACTCCTGCT-3′. Real-time PCR reactions were then performed in a total volume of 25 μl including 100 ng of the cDNA template, 12.5 μl of QuantiFast SYBR green PCR master mix, and the final concentration of primers of 0.5 μM. The PCR conditions were as follows: an initial step at 95 °C for 5 min, followed by 35 cycles of 10 s at 95 °C, 30 s at 60 °C, and 30 s at 72 °C. Fluorescence intensity was measured during the annealing step on an ABI-Prism 7300 analytical thermal cycler (Applied Biosystems). The RT-PCR data were analyzed according to the $2^{-\Delta\Delta C}{}_T$ method [14], and normalized by β-Actin mRNA expression in each sample. Experiments were performed in triplicate.

2.10. Western blot analysis

MDA-MB-231 cells treated with RAPTA-EA1 (10 μM) were incubated at 37 °C for 48 h. The cells were collected, and the entire cell extract was separated on a SDS-polyacrylamide gel electrophoresis (6% SDS-PAGE) and subsequently subjected to Western blotting as described previously [6]. In brief, the chemiluminescent HRP substrate (ClarityTM Western ECL substrate, BioRad) was used for the development of the bands using a high-performance chemiluminescent film (Amersham HyperfilmTM ECL). For BRCA1, the primary antibody was a mouse monoclonal IgG1 antibody (BRCA1 (Ab1) Mouse (MS110)) (Calbiochem, EMD Millipore) at 1:1000 dilution. The secondary antibody was a HRP conjugated, goat anti-mouse IgG (HAF, R&D System) at 1:5000 dilution.

2.11. Combination treatment of RAPTA-EA1 with olaparib

The cytotoxic effects of RAPTA-EA1 and olaparib either alone at various concentrations (0–60 μM) or in combination (0.01–20 μM, at a constant ratio of 1:1) were examined in MDA-MB-231 and MCF-7 cells using the MTT assay [18]. Additive, antagonistic or synergistic interactions were assessed using the combination index (CI) with the Chou-Talalay method [28], calculated by CompuSyn program (ComboSyn, Inc.).

2.12. Statistical analysis

SPSS version 22.0 was used for statistical analysis. All values are expressed as mean ± standard error of the mean (SEM) comparisons between two groups conducted by One-way ANOVA. Group differences resulting in $^*p < 0.01$ were considered statistically significant.

3. Results

3.1. Cytotoxic effect of RAPTA-EA1 on MDA-MB-231 breast cancer cells

The cytotoxicity effect of RAPTA-EA1 on MDA-MB-231 breast cancer cells was performed by a MTT assays, using cisplatin as a control. The results of the MTT assays are shown in Table 1. MDA-MB-231 cells were significantly more sensitive to RAPTA-EA1 than MCF-7 cells. The cytotoxicity of RAPTA-EA1 was found to be much higher ($IC_{50} = 10.5 \pm 0.5$) than that of cisplatin ($IC_{50} = 128.0 \pm 3.0$) in MDA-MB-231 cells. Therefore, we used the concentration of RAPTA-EA1 at its approximate IC_{50} value (10 μM) to perform all further experiments.

3.2. RAPTA-EA1 uptake into MDA-MB-231 cells blocks G2/M cell cycle and induces nuclear condensation leading to apoptosis

The ruthenium content in the MDA-MB-231 cells following treatment with RAPTA-EA1 (10 μM) for 48 h was determined using Inductive Coupled Plasma Mass Spectrometry (ICP-MS). The ruthenium was distributed in the nuclear fraction (43%), cytoplasm (30%), and mitochondria (27%) of the MDA-MB-231 cells (Figure 2A). In a previous study RAPTA-EA1 was shown to accumulate in the nuclear fraction and cytoplasm of MCF-7 cells and in the cytoplasm and mitochondrial fraction of HCC1937 cells [18].

3.3. Cellular BRCA1 damage, expression of BRCA1 mRNA and its protein in MDA-MB-231 cells

To assess cellular BRCA1 damage, MDA-MB-231 cells were treated with RAPTA-EA1 over a wide concentration range (0–100 μM) and following incubation for 48 h their genomic DNA was extracted. A PCR-based assay was used to quantitate the lesion frequencies induced by RAPTA-EA1 in the BRCA1 gene (3,426-bp fragment of the BRCA1 exon 11) of the MDA-MB-231 cells. The PCR products of ruthenated DNA indicate the polymerization of DNA in the specified BRCA1 [14]. The percentage of BRCA1 amplification as a function of RAPTA-EA1 concentration is shown in Figure 4A, with the growth of the BRCA1 gene decreasing as the RAPTA-EA1 concentration increases. The amplification of the BRCA1 gene decreased by 20% in the concentration range 10–100 μM (Figure 4A). Induction of lesions with the BRCA1 exon 11 were calculated by assessing an irregular (Poisson) spread of injury [29], and the measure of lesions for each BRCA1 fragment were estimated using the Poisson equation [29, 30], with approximately one lesion per BRCA1 fragment in the cells at 20% inhibition of DNA amplification, see Figure 4B.

The expression of BRCA1 mRNA and its protein in RAPTA-EA1-treated MDA-MB-231 cells was determined using real-time quantitative RT-PCR and Western blot analysis. RAPTA-EA1 suppresses the expression of BRCA1 mRNA in MDA-MB-231 cells (Figure 5A and B). Notably, BRCA1 expression was reduced by almost 50 % compared to the untreated control cells (Figure 5C).

3.4. Combination treatment of olaparib and RAPTA-EA1

MDA-MB-231 cells are approximately 2-fold less susceptible to olaparib compared to MCF-7 cells (Figure 6A and B), while RAPTA-EA1 is perfectly suppressed the viability of both cells at the same concentration (Figure 6C and D). The combination of olaparib (10 μM) and RAPTA-EA1 (10 μM) results in a combination index (CI) of 0.24 (potent synergy) in MCF-7 cells and 0.78 (almost additive) in MDA-MB-231 cells (Figure 6E and F). Olaparib downregulates the expression of BRCA1 mRNA in MDA-MB-231 cells, whereas it is upregulated in MCF-7 cells. However, the combined inhibitors induce overexpression of BRCA1 mRNA in both cells (Figure 7A, B and C). The expression level of the BRCA1 protein is dramatically reduced after treatment with the olaparib-RAPTA-EA1 combination, compared with the untreated controls (Figure 7D, E and F).

Table 1. Cytotoxicity of MDA-MB-231 and MCF-7 cells induced by IC_{50} values (μM) of RAPTA-EA1 and cisplatin using the MTT assay after 48 h of treatment (data reflect the mean and ±SEM of results from three separate experiments, each performed in triplicate).

Compound	IC_{50} (μM)	
	MDA-MB-231	MCF-7
RAPTA-EA1	10.5 ± 0.5*,**	20.0 ± 2.2*,**
cisplatin	128.0 ± 3.0*,**	42.0 ± 2.0*,**

Statistically significant differences are indicated by $*p < 0.01$, compared the IC_{50} values of the same compound on cell lines, and $**p < 0.01$, compared the IC_{50} values of the same compounds on each cell line. All experiments were performed in triplicate.

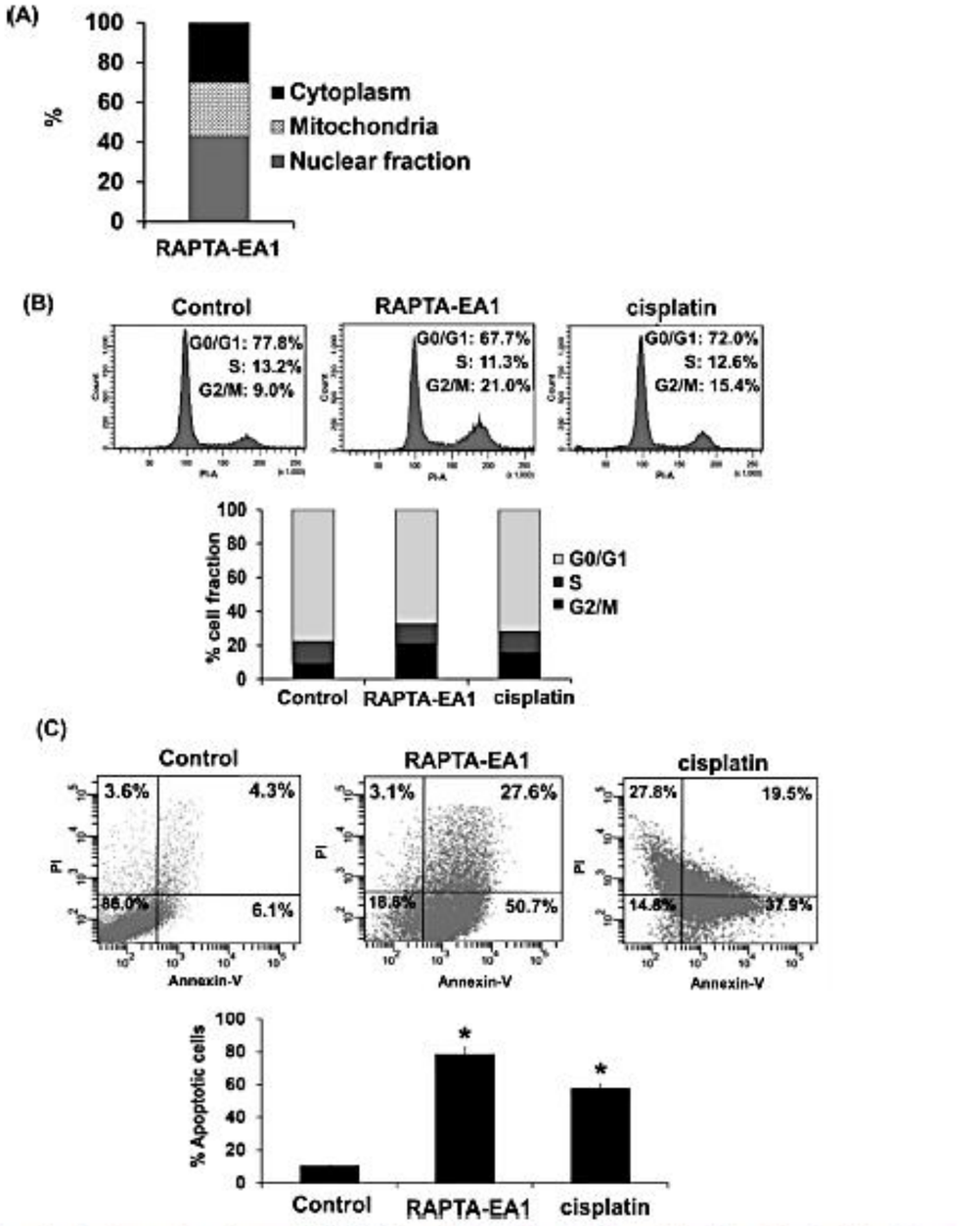

Figure 2. Cellular uptake, cell cycle progression, and apoptosis of RAPTA-EA1-treated MDA-MB-231 cells. (A) Accumulation and distribution of ruthenium in breast cancer cell lines were treated with RAPTA-EA1 at the IC_{50} concentration (10 μM) at 37 °C for 48 h. The distribution of ruthenium was determined in the nuclear fraction, mitochondria and cytoplasm using ICP-MS. (B) Quantification of DNA by PI staining after treatment of the cells with RAPTA-EA1 (10 μM) or the IC_{50} concentration of cisplatin (128 μM) (Table 1) at 37 °C for 48 h. FACS (fluorescence-activated cell sorting) was used to investigate the proportion of cells arrested at multifarious phases of the cell cycle. Each experiment used 20,000 cells. (C) Determination of starting apoptotic cells (Annexin V-positive/PI-negative) and late apoptosis cells (Annexin V-positive/PI-positive) following incubation with RAPTA-EA1 (10 μM) or cisplatin (128 μM) at 37 °C for 48 h. Flow cytometric analysis was used to measure cells that bind Annexin V-FITC and PI apoptosis staining. Experiments were performed in triplicate and the bar represents the standard error (*$p < 0.01$).

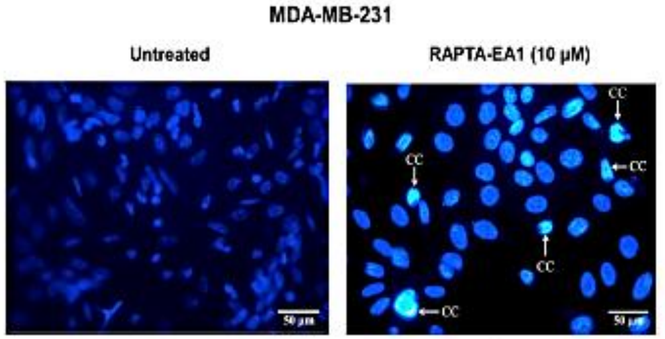

Figure 3. Immunofluorescence assay. Cells treated with RAPTA-EA1 (10 µM) were seeded on coverslips, fixed using 4% paraformaldehyde for 30 min and then permeabilized using 0.2% Triton X-100. The cells were incubated with blocking reagent for 1 h at ambient temperature and then their nuclei were treated with counterstaining, 4', 6-diamidino-2-phenylindole (DAPI; 1 µg/mL). CC stands for chromatin condensation.

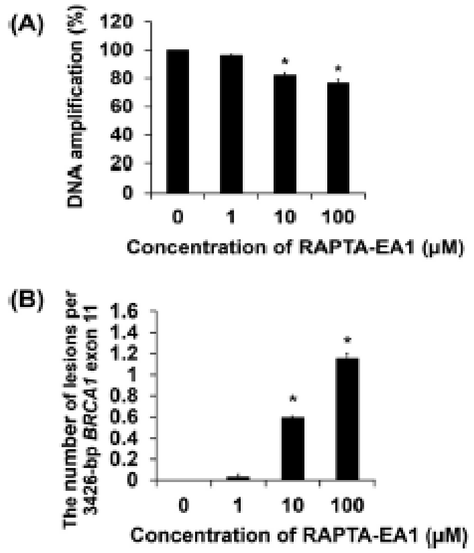

Figure 4. Cellular BRCA1 damage in MDA-MB-231 cells. Cells were incubated with RAPTA-EA1 at different concentrations (0–100 µM) at 37 °C for 48 h. The fragment of BRCA1 was used as the DNA target which comprises 3426 bp located on BRCA1 exon 11. It was isolated from MDA-MB-231 cells, multiplied by PCR then the amplified DNA fragment was electrophoresed on 1% agarose gel. Staining was performed using ethidium bromide and imaged in the presence of ultraviolet light. The band intensity indicates the magnification of products quantified on a Bio-Rad Molecular Imager. The amount of DNA amplification (%) was plotted as a function of concentration (A). RAPTA-EA1-induced damaged BRCA1 fragment (lesions per the 3426-bp fragment) in MDA-MB-231 cells was calculated by the Poisson equation [14] (B). Experiments were performed in triplicate and the bar represents the standard error of experiments. Statistically significant differences from the untreated control cells are indicated by $^{*}p < 0.01$.

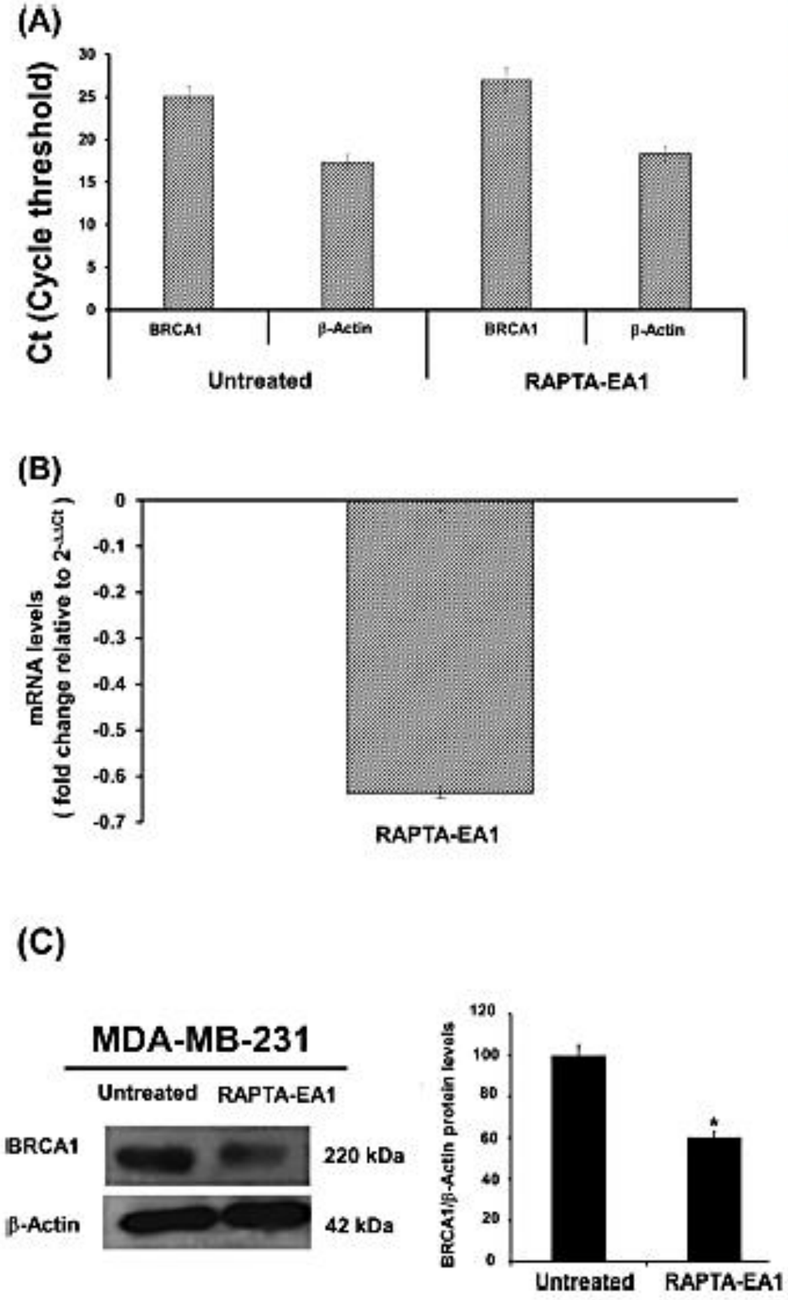

Figure 5. Effect of RAPTA-EA1 on the expression of BRCA1 mRNA and its protein in MDA-MB-231 cells. The transcribed BRCA1 gene was quantified by RT-PCR, normalized to the reference gene β-Actin and treatment-free control cells (A, B). Data were calculated using the $2^{-\Delta\Delta C_T}$ method [14]. Protein expression was performed by Western blot analysis (C and SI-Fig. 1). Experiments were performed in triplicate and the bar represents the standard experimental errors. Statistically significant differences from the untreated control cells are indicated by $^{*}p < 0.01$.

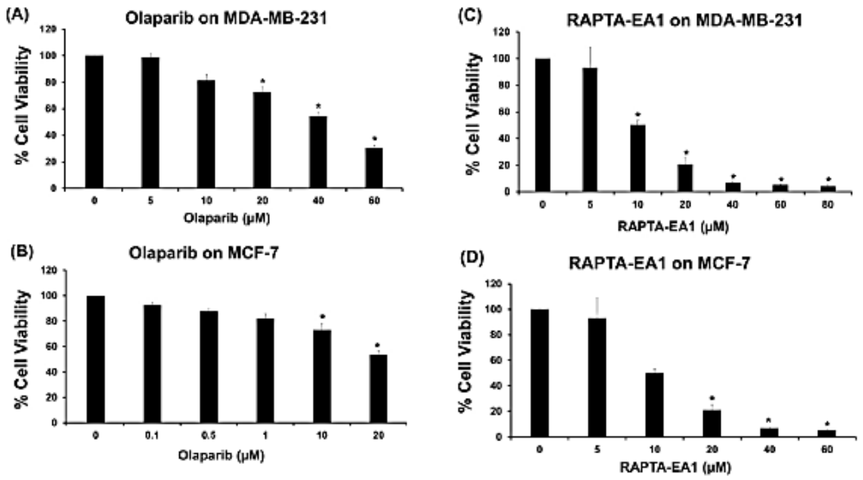

Figure 6. The cell growth inhibitory effect of olaparib alone and in combination with RAPTA-EA1. MDA-MB-231 and MCF-7 cells were treated with various concentrations of olaparib (A, B), RAPTA-EA1 (C, D) or olaparib in combination with RAPTA-EA1 (E, F) for 48 h at 37 °C. Experiments were performed in triplicate and the bar represents the standard experimental errors. Statistically significant differences were considered $^{*}p < 0.01$. Entering a series of "dose (D) and effect (Fa)" into computer for each drug alone and their combinations, the software will automatically simulates the CI values at different Fa levels in seconds, based on the CI algorithm. This plot is called the Fa-CI plot or the Chou-Talalay plot, calculated by CompuSyn program (ComboSyn, Inc.) (E, F).

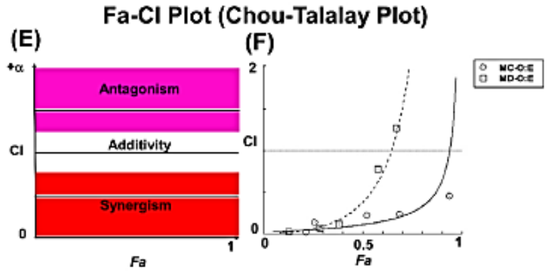

MC-O:E is the combination of olaparib+RAPTA-EA1 on MCF-7 cell
MD-O:E is the combination of olaparib+RAPTA-EA1 on MDA-MB-231 cell

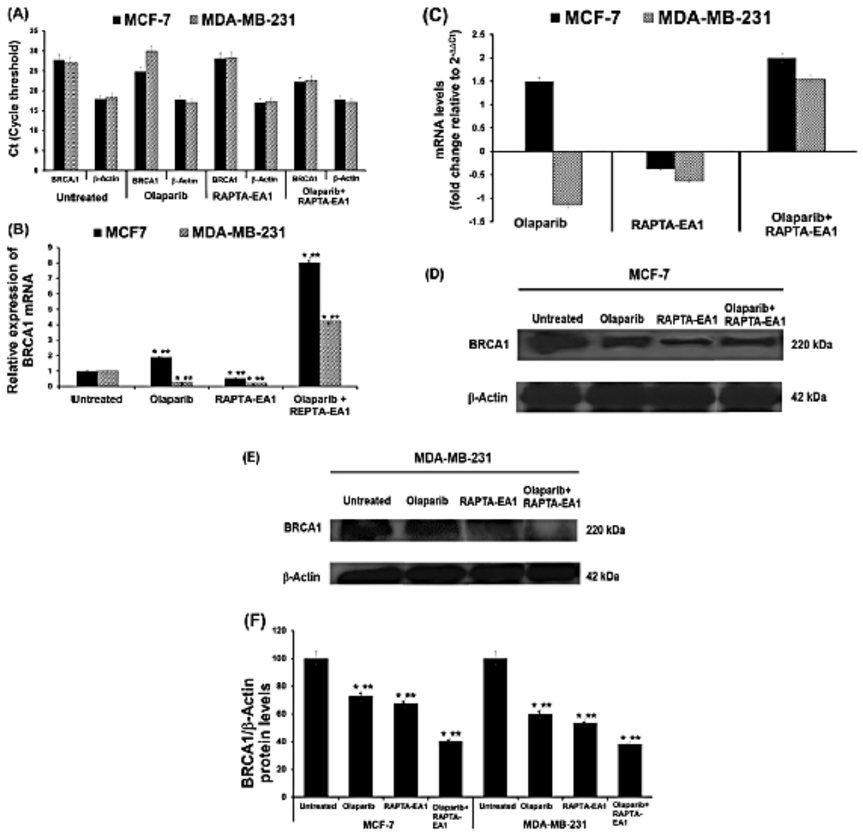

Figure 7. Differential expression of the BRCA1 mRNA and its protein. The amount of transcribed BRCA1 genes was determined quantitatively using RT-PCR, β-Actin expression was used as the normalized gene, compared to the untreated control cells. Data were analyzed according to the $2^{-\Delta\Delta C_T}$ method [14]. Experiments were performed in triplicate. A: cycle threshold (Ct) for each sample, B: relative expression of BRCA1 mRNA, C: fold change for BRCA1 mRNA between MCF-7 and MDA-MB-231 sample. D-E (SI-Fig. 2), and F: Western-blot analysis of BRCA1 protein expression in cells treated with olaparib, RAPTA-EA1 and olaparib-RAPTA-EA1 combination. In all experiments cells were harvested after 48 h treatment. $^{*}p < 0.01$, compared the expression of the BRCA1 mRNA or its protein on each cell line treated by single or combination treatment in untreated control cells, and $^{**}p < 0.01$, compared the expression of the BRCA1 mRNA or its protein treated by the same.

4. Discussion

This study provides further mechanistic insights on the mode of action of RAPTA-EA1, a ruthenium-based GSTP-1 inhibitor, for the treatment of triple-negative BRCA1-competent MDA-MB-231 breast cancer cells. Following cellular uptake, RAPTA-EA1 accumulates mostly in the nuclear fraction of MDA-MB-231 cells. Moreover, RAPTA-EA1 induces an irreversible, anomalous state of condensed chromatin, ruthenium-adducts in the specific nucleosome core, which blocks the binding of a key protein for nuclear factor association and chromatin condensation inducing alterations in chromatin fiber folding [31]. This association generates substantial of mitotic cell death at the G2/M phase of the cell cycle progression [32]. The evidence suggests that cellular DNA damage triggers the inactivation of phosphorylation to cyclin-dependent kinase CDK1-cyclin B1 complex, which leads to cell death through G2/M checkpoint deregulation [32].

It has previously been shown that RAPTA-EA1 triggers multi-mechanistic pathways including programed cell death and regulation of JNK signaling by GSTp [33, 34]. Some evidence indicates that ruthenium-based complexes induce DNA destruction that halts the DNA replication as well as transcription with a similar kinetic to cisplatin [35]. Therefore, we analyzed the DNA destruction in vitro on the BRCA1 gene treated with RAPTA-EA1 and found that the compound damages BRCA1 and subsequently decreases BRCA1 replication in MDA-MB-231 cells. These findings are similar to those previously obtained in triple-negative, BRCA1-mutant HCC1937 cells and sporadic BRCA1-wild type MCF-7 cells [18]. RAPTA-EA1 inhibits BRCA1 replication in HCC1937 cells to a greater extent than in MCF-7 cells [18]. However, the level of inhibition of BRCA1 replication by RAPTA-EA1 in MDA-MB-231 cells was considerably lower. This may be, in part, due to mutual interaction between ranted. It seems that drug susceptibility in triple-negative BRCA1 wild-type breast cancer MDA-MB-231 cells is linked to the reduced expression of the BRCA1 protein in repairing DNA damage after RAPTA-EA1 exposure. Olaparib targets PARP1, a DNA repair protein, leading to cell death via synthetic lethality [50] when applied in combination in RAPTA-EA1.

Declarations

Author contribution statement

Khwanjira Hongthong: Performed the experiments; Analyzed and interpreted the data; Wrote the paper.

Tidarat Nhukeaw, Pornvichai Temboot: Performed the experiments; Analyzed and interpreted the data.

Paul J. Dyson: Contributed reagents, materials, analysis tools or data; Wrote the paper.

Adisorn Ratanaphan: Conceived and designed the experiments; Analyzed and interpreted the data; Contributed reagents, materials, analysis tools or data; Wrote the paper.

Funding statement

This work was supported by the National Research Council of Thailand and Prince of Songkla University (PHA570058S, PHA580500S, PHA610093S-1, and PHA6202079S), the Thailand Research Fund under the Royal Golden Jubilee Ph.D. Program (to Pornvichai Temboot, 5.G.PS/49/F.2), and the Prince of Songkla University Scholarship for Ph.D. Program (to Khwanjira Hongthong, PSU 0919/2552) and (to Tidarat Nhukeaw, PSU 019/2557).

Data availability statement

Data included in article/supplementary material/referenced in article.

Declaration of interests statement

The authors declare no conflict of interest.

Additional information

Supplementary content related to this article has been published online at https://doi.org/10.1016/j.heliyon.2021.e07749.

Acknowledgements

We wish to thank Dr. Brian Hodgson and Ms. Korawan Chakree for technical assistance. We are grateful to the Pharmaceutical Laboratory Service Center, Faculty of Pharmaceutical Sciences, Prince of Songkla University for research facilities.

References

[1] M.L. Plasilova, B. Hayse, B.K. Killelea, N.R. Horowitz, Features of triple-negative breast cancer: analysis of 38,813 cases from the national cancer database, Medicine (Baltim). 95 (2016), e4614.

[2] M. Tian, Y. Zhong, F. Zhou, Z. Liao, Platinum-based therapy for triple-negative breast cancer treatment: a meta-analysis, Mol. Clin. Oncol. 3 (2015) 720–724.

[3] G. Ciarimboli, Membrane transporters as mediators of cisplatin side-effects, Anticancer Res. 34 (2014) 547–550.

[4] A. Dorcier, P.J. Dyson, C. Gossens, U. Rothlisberger, R. Scopelliti, I. Tavernelli, Binding of organometallic ruthenium(II) and osmium(II) complexes to an oligonucleotide: A combined mass spectrometric and theoretical study, Organometallics 24 (2015) 2114–2123.

[5] C. Scolaro, A. Bergamo, L. Brescacin, R. Delfino, M. Cocchietto, G. Laurenczy, J. Geldbach T, G. Sava, P.J. Dyson, In vitro and in vivo evaluation of ruthenium(II)-arene PTA complexes, J. Med. Chem. 48 (2005) 4161–4171.

[6] P. Nowak-Sliwinska, T. Segura, M.L. Iruela-Arispe, The chicken chorioallantoic membrane model in biology, medicine and bioengineering, Angiogenesis 17 (2014) 779–804.

[7] G. Süss-Fink, Arene ruthenium complexes as anticancer agents, Dalton Trans. 39 (2010) 1673–1688.

[8] T. Nhukeaw, K. Hongthong, P.J. Dyson, A. Ratanaphan, Cellular responses of BRCA1-defective HCC1937 breast cancer cells induced by the antimetastasis ruthenium(II) arene compound RAPTA-T, Apoptosis 24 (2019) 612–622.

[9] F. Battistin, F. Scaletti, G. Balducci, S. Pillozzi, A. Arcangeli, L. Messori, E. Alessio, Water-soluble Ru(II)- and Ru(III)-halide-PTA complexes (PTA=1,3,5-triaza-7-phosphaadamantane): chemical and biological properties, J. Inorg. Biochem. 160 (2016) 180–188.

[10] S. Chatterjee, S. Kundu, A. Bhattacharyya, C.G. Hartinger, P.J. Dyson, The ruthenium(II)-arene compound RAPTA-C induces apoptosis in ECA cells through mitochondrial and p53-JNK pathway, J. Biol. Inorg. Chem. 13 (2018) 1149–1155.

[11] P. Temboot, R.F.S. Lee, L. Menin, L. Patiny, P.J. Dyson, A. Ratanaphan, Biochemical and biophysical characterization of ruthenation of BRCA1 RING protein by RAPTA complexes and its E3 ubiquitin ligase activity, Biochem. Biophys. Res. Commun. 488 (2017) 355–361.

[12] W.H. Ang, L.J. Parker, A. De Luca, L. Juillerat-Jeanneret, C.J. Morton, M. Lo Bello, M.W. Parker, P.T. Dyson, Rational design of an organometallic glutathione transferase inhibitor, Angew Chem. Int. Ed. Engl. 48 (2009) 3854–3857.

[13] S.M. Louie, E.A. Grossman, L.A. Crawford, L. Ding, R. Camarda, T.R. Huffman, D.K. Miyamoto, A. Goga, E. Weerapana, D.K. Nomura, GSTP1 Is a driver of triple-negative breast cancer cell metabolism and pathogenicity, Cell. Chem. Biol. 23 (2016) 567–578.

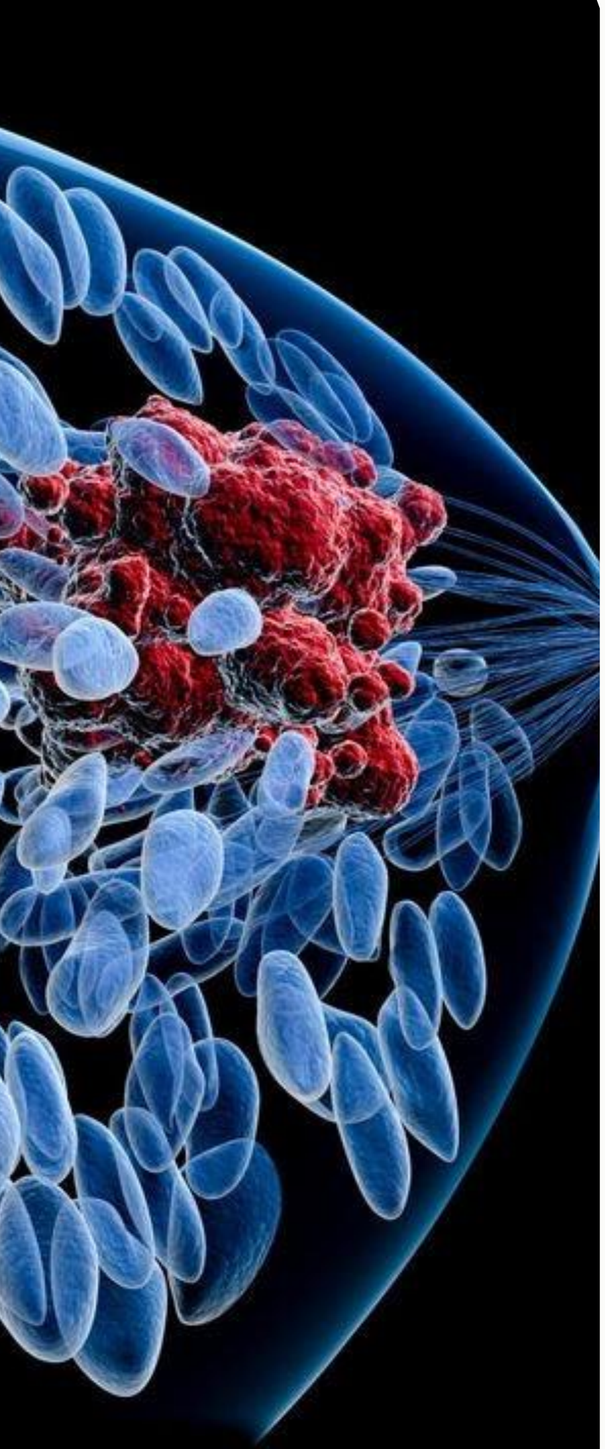

HELIYON 7 (2021) E07749

ANTICANCER ACTIVITY OF RAPTA-EA1 IN TRIPLE-NEGATIVE BRCA1 PROFICIENT BREAST CANCER CELLS: SINGLE AND COMBINED TREATMENT WITH THE PARP INHIBITOR OLAPARIB

Khwanjira Hongthong, Tidarat Nhukeaw, Pornvichai Temboot, Paul J. Dyson, Adisorn Ratanaphan

Asst. Prof. Dr. Gulsiri Senawong

Department of Biochemistry, Faculty of Science, Khon Kaen University

Breast cancer

The Globalcan 2020

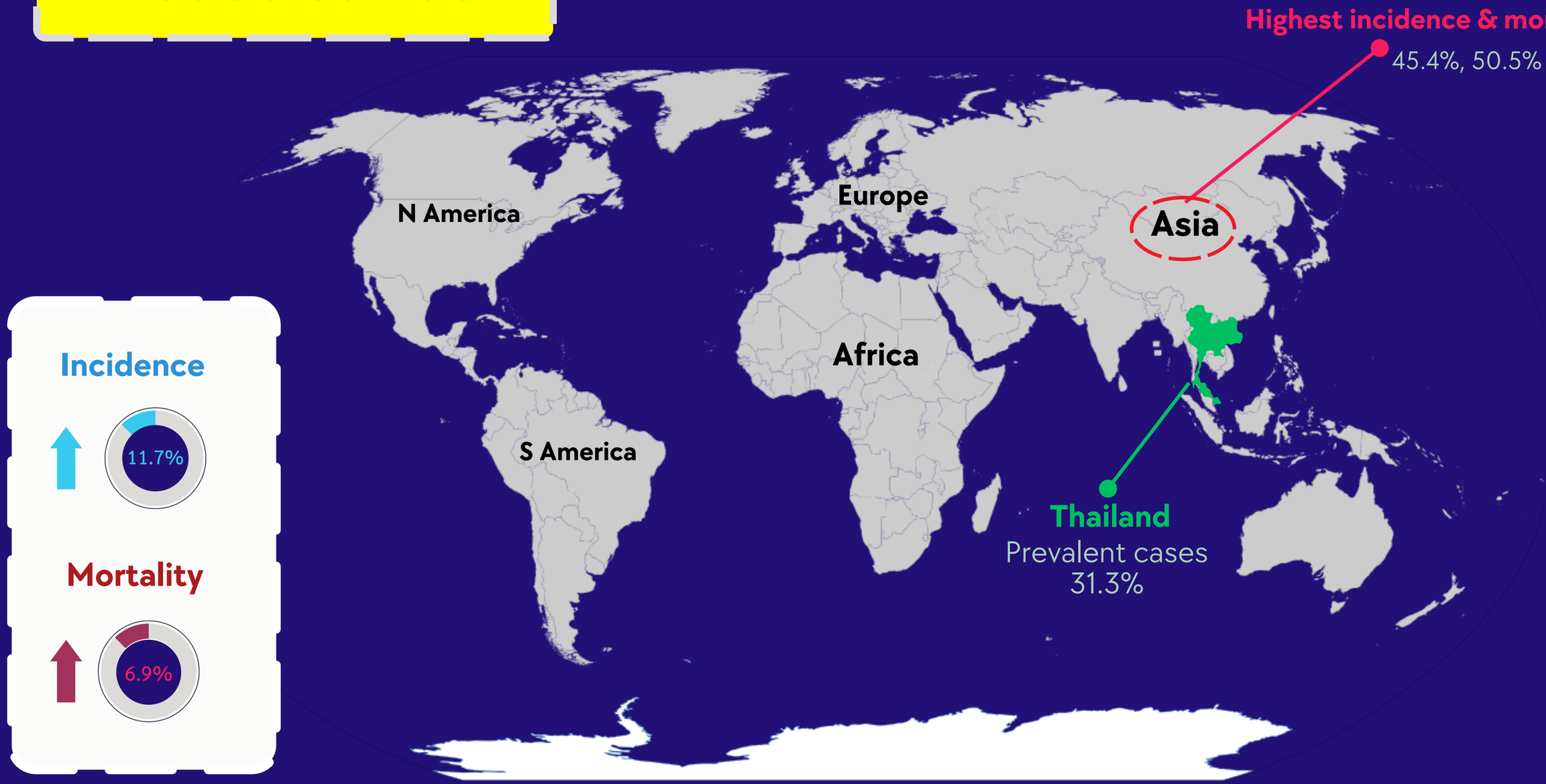

Breast Cancer Subtypes

*Classification based on expression of hormone receptors

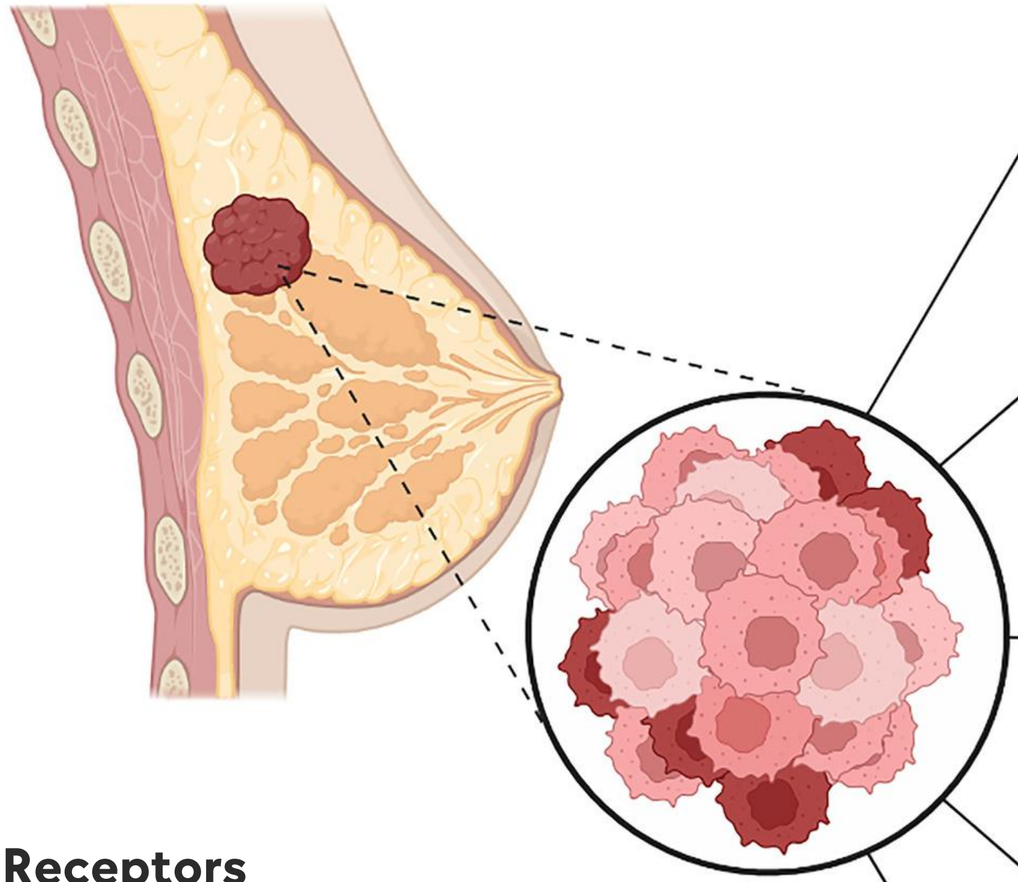

Luminal A (~40%)
ER+, PR+, HER2-

Normal-like (~2-8%)
ER+, PR+, HER2-

Luminal B (~20%)
ER+, PR+, HER2+/-

HER2-enriched (~10-15%)
HER2+

Triple-negative (~15-20%)
ER-, PR-, HER2-

Receptors

ER = Estrogen

PR = Progesterone

HER2 = Human epidermal growth factor receptor 2

Triple-negative/ TNBC/ Basal-like


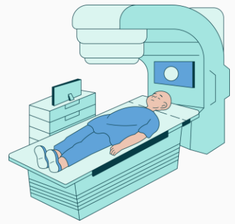


No hormone receptor expression

~~ER, PR, HER2~~

Response to chemotherapy

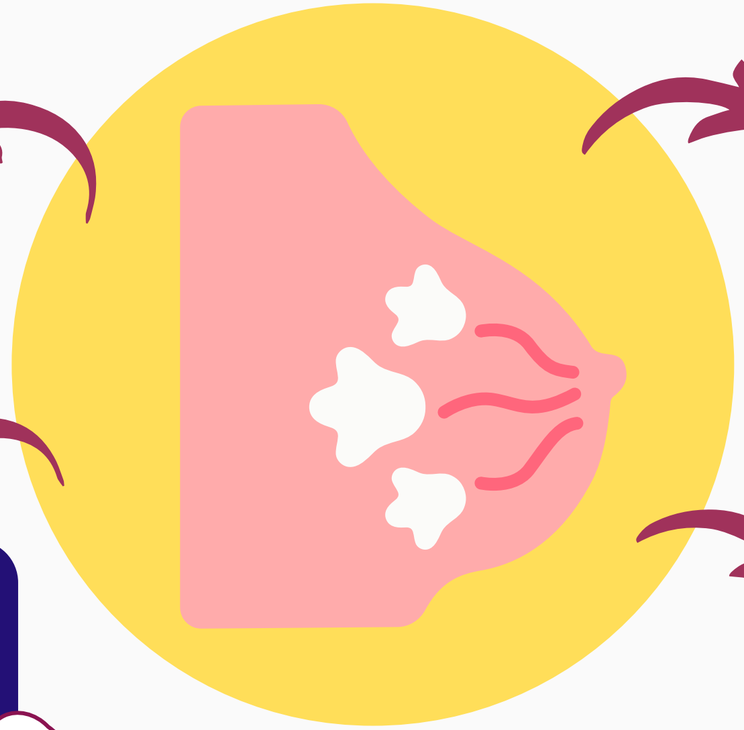

TNBC patients

- Hard to detect
- High recurrence and spread rate
- Low survival rate

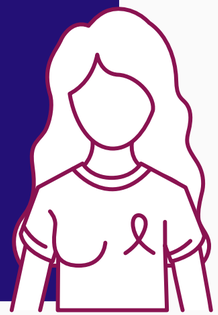

Difficult to treat


Platinum-based drugs

Advantage:

- Can inhibit cancer cells that are rapidly dividing

Cisplatin

Disadvantage:

- Induce secondary mutations
- Acquired drug resistance
- High general toxicity (*e.g.* hepatotoxicity)
- Expensive

Ruthenium-based drugs

Arene-ruthenium (II)-complexes containing PTA (1,3,5-tri-aza-7-phosphaadamantane), often termed RAPTA

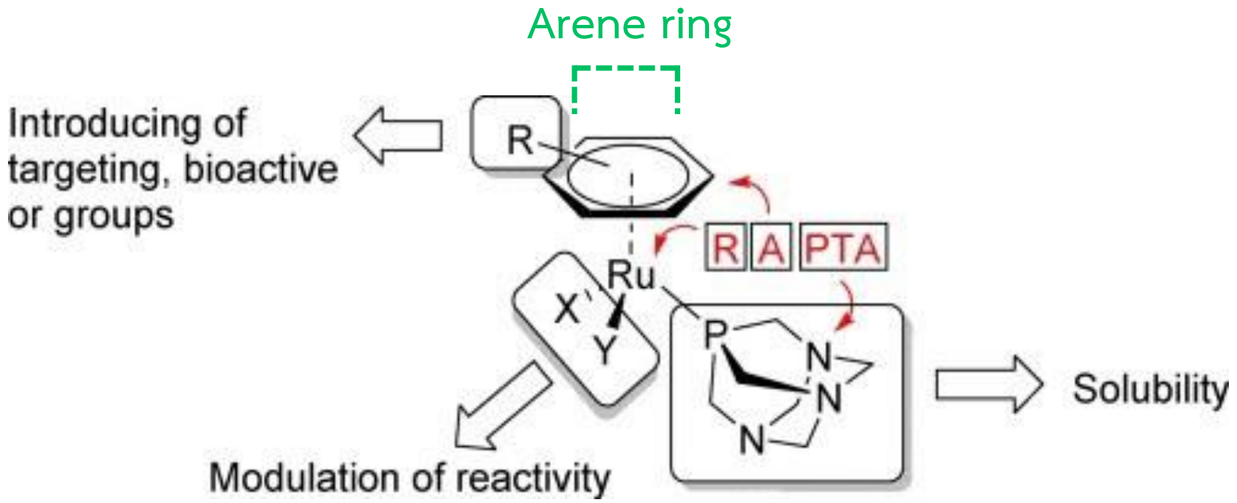

RAPTA-EA1

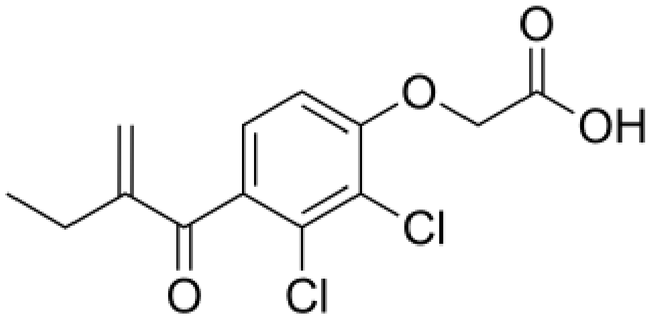

Ethacrynic acid (EA)

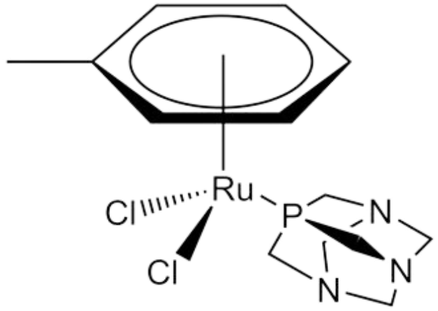

RAPTA compound

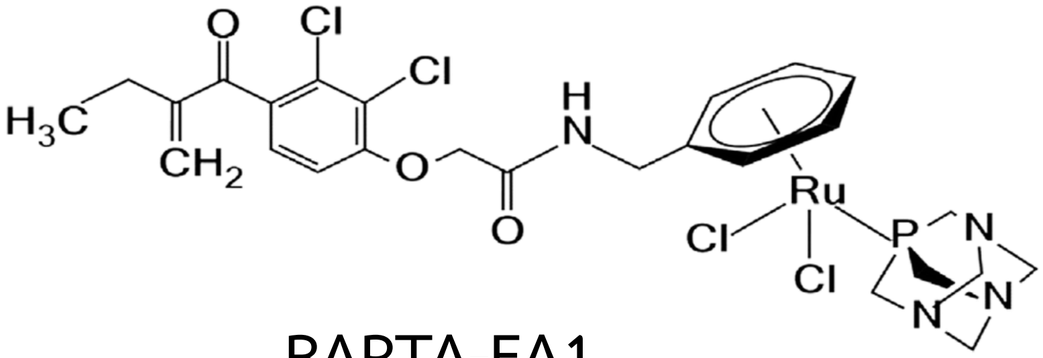

RAPTA-EA1

- RAPTA compound with ethacrynic acid tethered to the arene ring, termed RAPTA-EA1
- Strong inhibitor of glutathione-S-transferase P1 (GSTP-1)

Objectives

- To evaluate anticancer efficacy of RAPTA-EA1 against triple-negative BRCA1 wild-type breast cancer (MDA-MB-231) cells through BRCA1 inhibition

- To evaluate the combined treatment of PARP inhibitor (Olaparib) with RAPTA-EA1 in MDA-MB-231 cells and in sporadic BRCA1 wild-type MCF-7 cells

SCOPE OF STUDY

Cytotoxicity effect of RAPTA-EA1 on MDA-MB-231 and MCF-7 cells

- MTT proliferation assay

Uptake of RAPTA-EA1 and molecular mechanism of anticancer activity of RAPTA-EA1 in MDA-MB-231 cells

- Cellular accumulation and distribution
- Cell cycle analysis
- Apoptosis detection by Annexin V
- Immunofluorescence assay

Cellular BRCA1 damage, expression of BRCA1 mRNA and its protein in MDA-MB-231 cells

- Utilization of Quantitative PCR (qPCR) for cellular BRCA1 damage
- Reverse transcription quantitative real-time PCR (RT-qPCR)
- Western blot analysis

Combination treatment of olaparib and RAPTA-EA1

- MTT assay, RT-qPCR, Western blotting

Materials

RAPTA-EA1 — Preparing by literature method

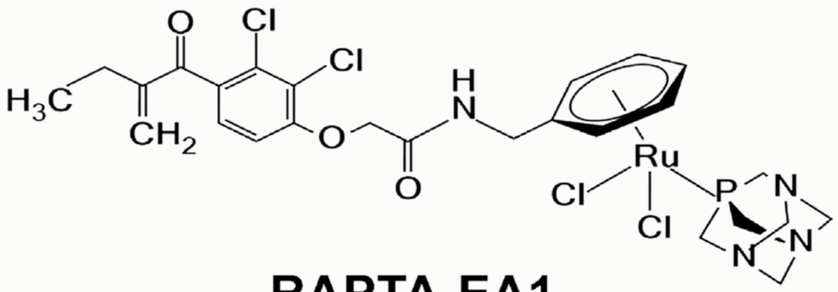

RAPTA-EA1

Cisplatin — Sigma-Aldrich (USA)

Prepare stock solution (1-5 μM) in deionized water

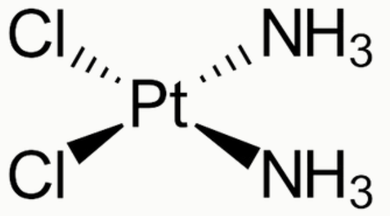

Olaparib — Prepare stock solution (0-60 μM)

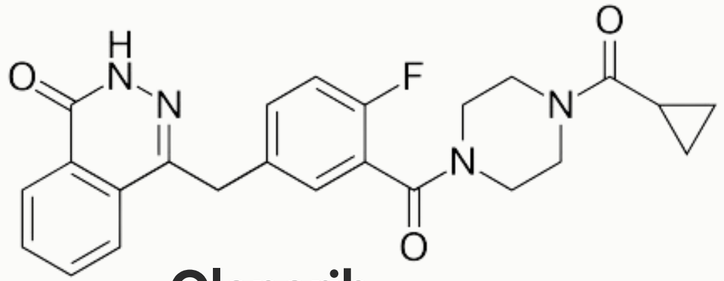

Olaparib

Cell culture

MDA-MB-231 cells

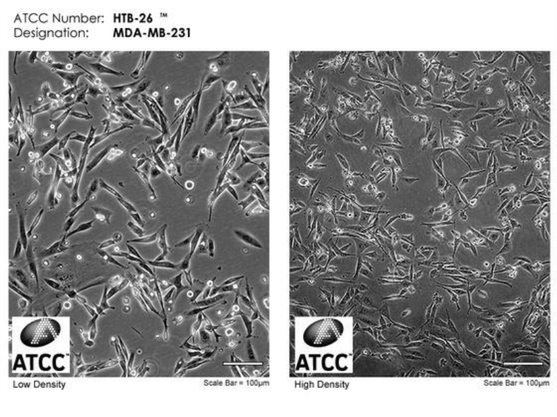

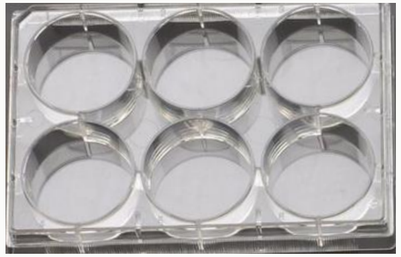

Human breast cancer cell lines → **Seed in 6-well plate** → **Cell were incubated**

MCF-7 cells

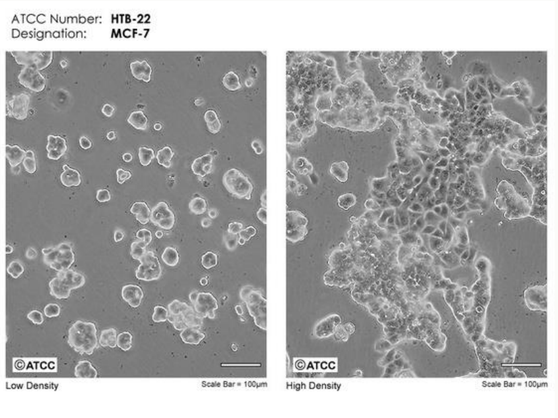

Conditions:

- DMEM medium without phenol red
- 10% FBS
- 1% penicillin-streptomycin

Conditions:

- At 37°C
- 5% CO_2

MTT proliferation assay

Seeding density

5x10^4 cells of
MDA-MB-231 and MCF-7

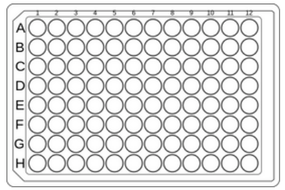

Cultured cells

in 96 well plate

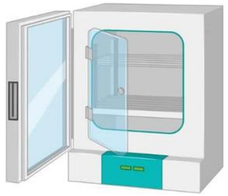

Incubated

at 37°C, 48 h., 5% CO_2

RAPTA-EA1
(various conc.)

Cisplatin

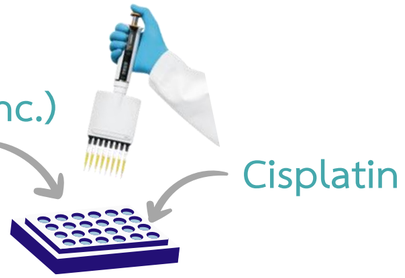

Removed and added fresh culture medium

Incubated 48 h.

Washed twice

With 1XPBS

*MTT is light sensitive

Incubated 4 h.

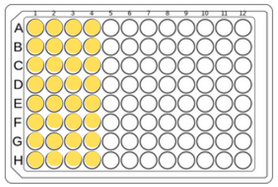

Added MTT solution

Gently removed medium

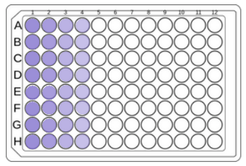

Added DMSO

Measured absorbance at 570 nm

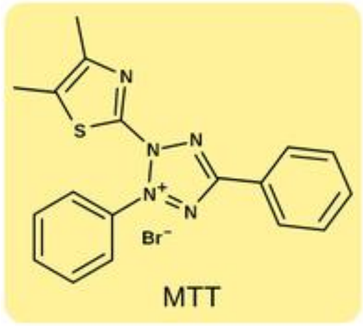

MTT

Mitochondrial Reductase

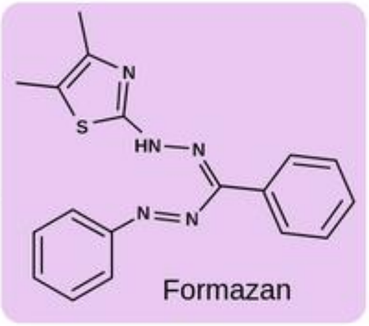

Formazan

Results

Table 1. Cytotoxicity of MDA-MB-231 and MCF-7 cells induced by IC_{50} values (μM) of RAPTA-EA1 and cisplatin using the MTT assay after 48 h. of treatment (data reflect the mean and ± SEM of results from three separate experiment, each preformed in triplicate)

Compound	IC_{50} (μM)	
	MDA-MB-231	MCF-7
RAPTA-EA1	10.5 ± 0.5*,**	20.0 ± 2.2*,**
cisplatin	128.0 ± 3.0*,**	42.0 ± 2.0*,**

*IC_{50} is half-maximal inhibitory concentration

RAPTA-EA1 can inhibit the proliferation of MDA-MB-231 cells better than MCF-7 cells, while cisplatin can inhibit the proliferation of MCF-7 cells better than MDA-MB-231 cells.

Cellular accumulation and distribution

Seeding density

5x10^6 cells of MDA-MB-231

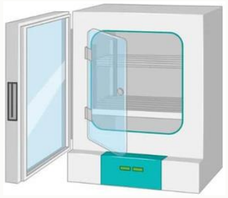

Incubated with RAPTA-EA1

at 37°C, 48 h., 5% CO_2

Washed twice

with PBS

Fractionated cells

ICP-MS

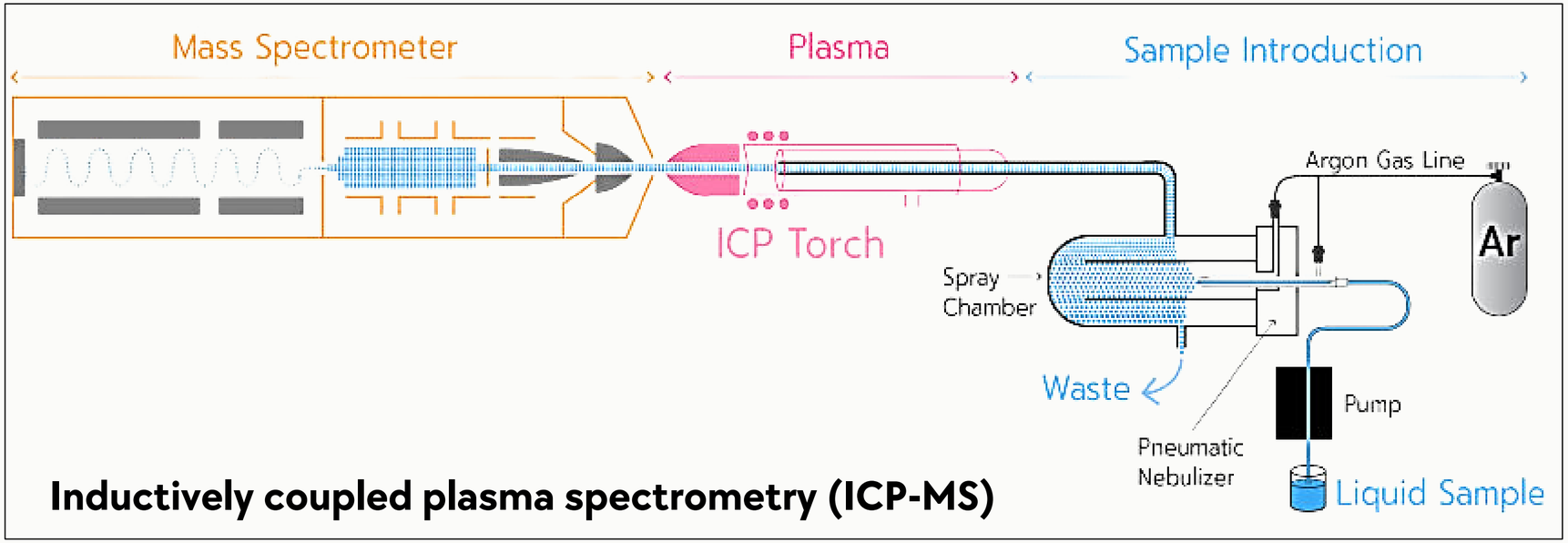

Inductively coupled plasma spectrometry (ICP-MS)

Results

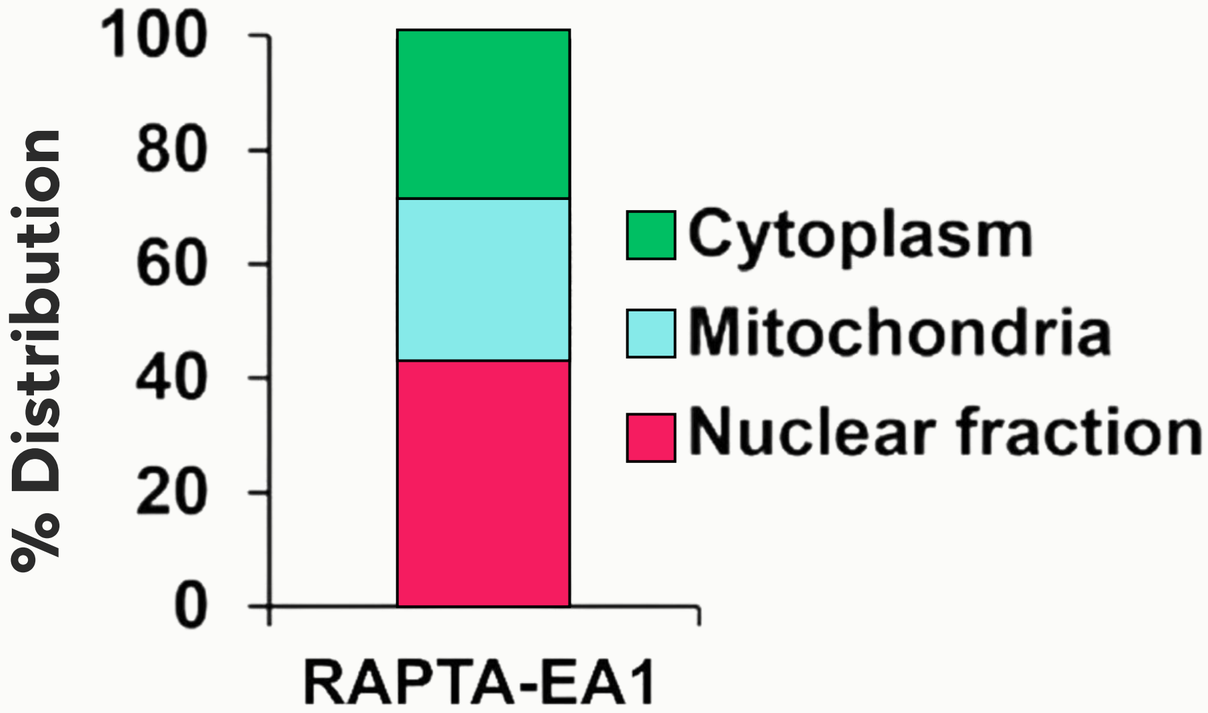

The ruthenium was distributed in the nuclear fraction 43%, cytoplasm 30% and mitochondria 27% of MDA-MB-231 cells.

Fig 1. Accumulation and distribution of ruthenium in breast cancer cell lines were treated with PAPTA-EA1 at the IC_{50} concentration (10 μM) at 37°C for 48 h. The distribution of ruthenium was determined in the nuclear fraction, mitochondria and cytoplasm using ICP-MS

Cell cycle analysis

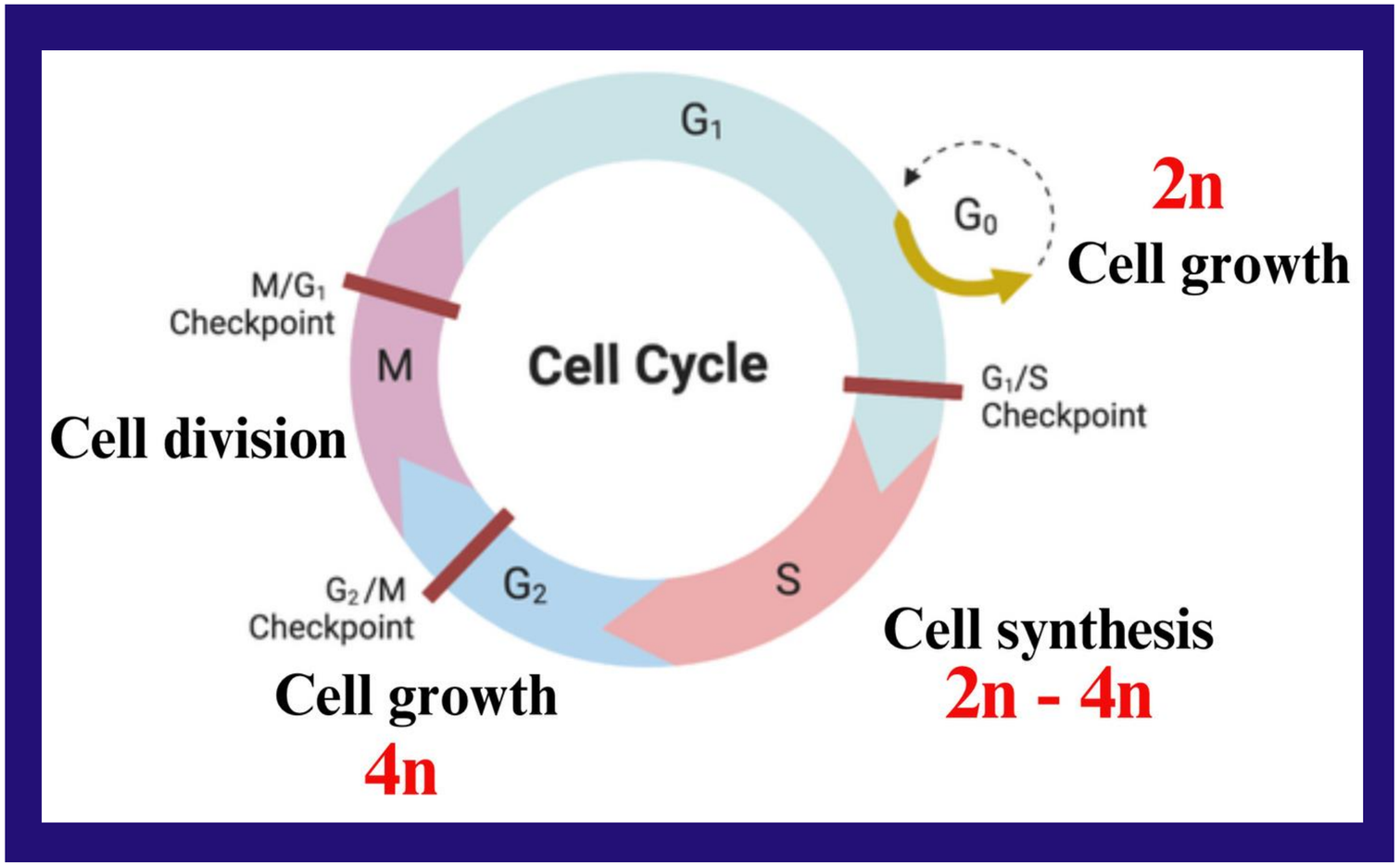

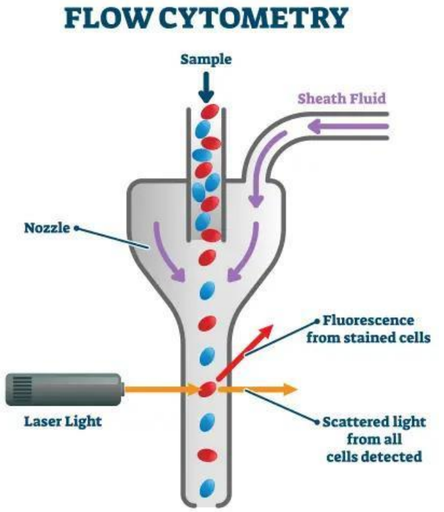

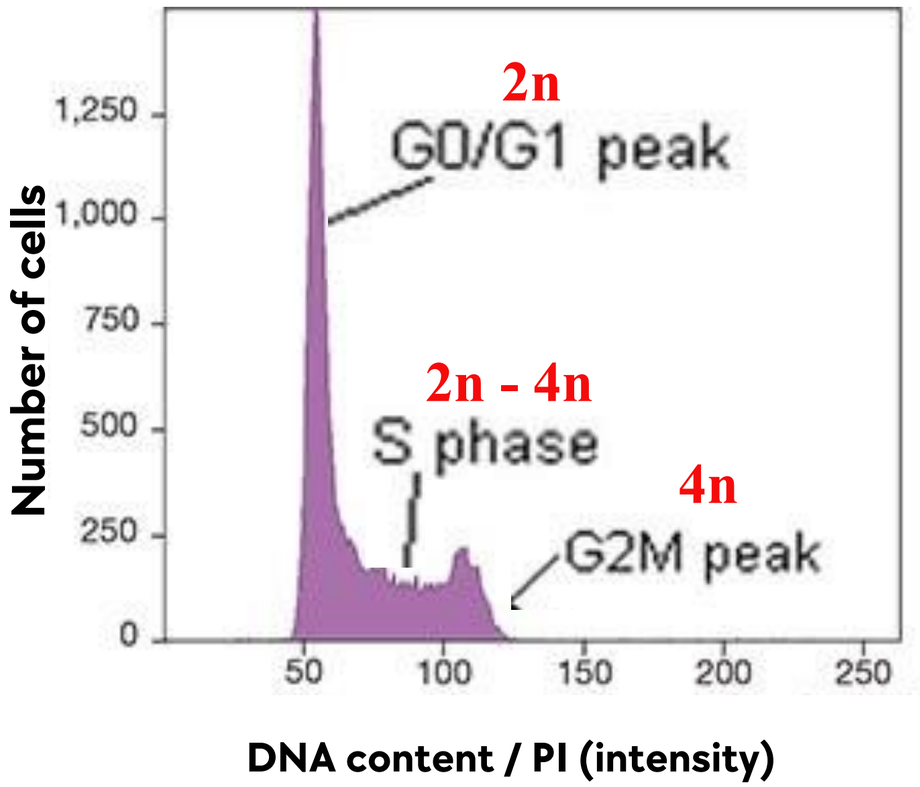

≈10^6 MDA-MB-231 cells

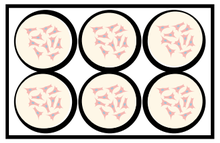

80% confluence

RAPTA-EA1 (10 µM)
or
Cisplatin (128 µM)

Incubated
at 37°C, 48 h., 5% CO_2

Trypsinized

0.25% trypsin
Washed with PBS
Centrifuged at 300g 5 min.

Collected & fixed
with cold ethanol (70%)

Stored overnight
at 20°C

Washed & re-suspended
PBS (1 mL)
RNase (100 µg/mL)
PI (50 µg/mL)
Triton-X-100 (0.1%)

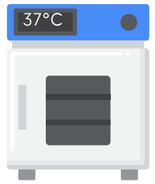

Incubated
at 37°C, 30 min.
in the dark

FACS canto
flow cytometer

Results

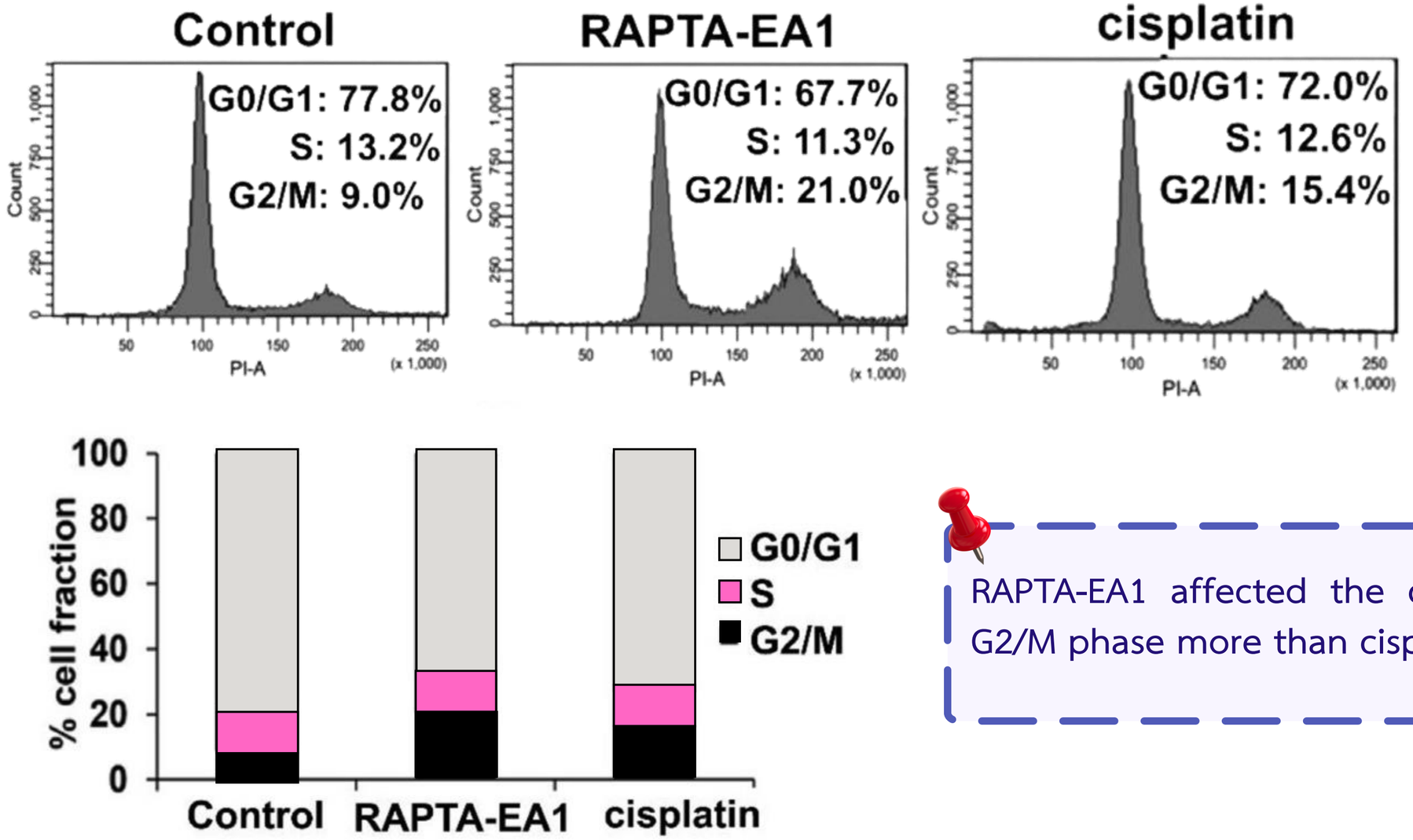

RAPTA-EA1 affected the cell cycle progression at G2/M phase more than cisplatin.

Fig 2. Quantification of DNA by PI staining after treatment of the cells with RAPTA-EA1 (10 μM) or the IC50 concentration of cisplatin (128 μM) **(Table 1)** at 37°C for 48 h. FACS (fluorescence-activated cell sorting) was used to investigate the proportion of cells arrested at multifarious phases of the cell cycle. Each experiment used 20,000 cells.

Apoptosis detection by Annexin V

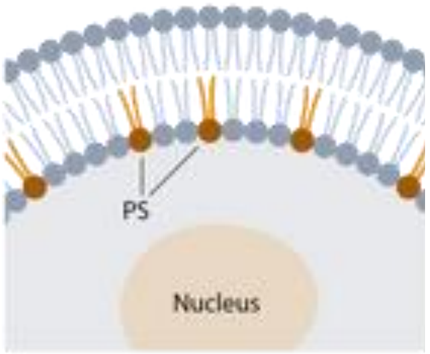

Healthy cell

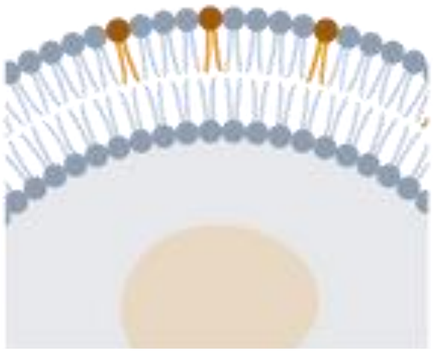

Apoptosis cell

Annexin V/
PI staining

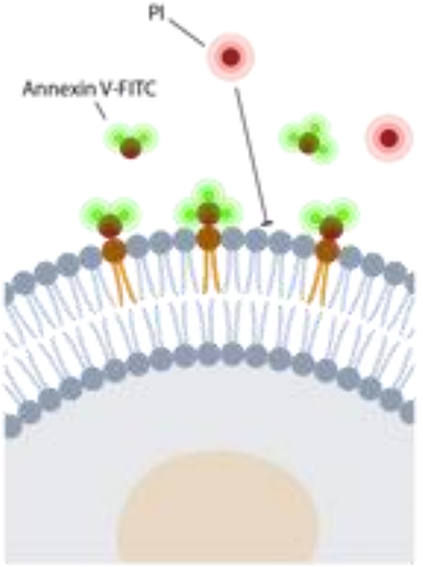

Early apoptosis

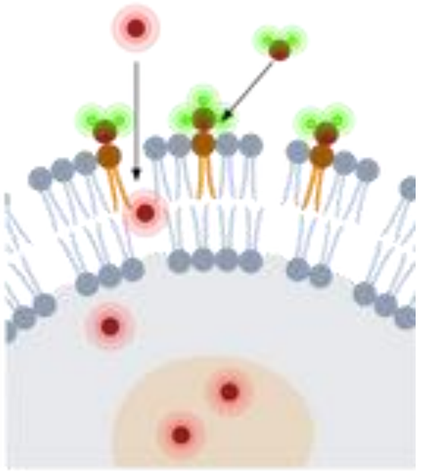

Late apoptosis

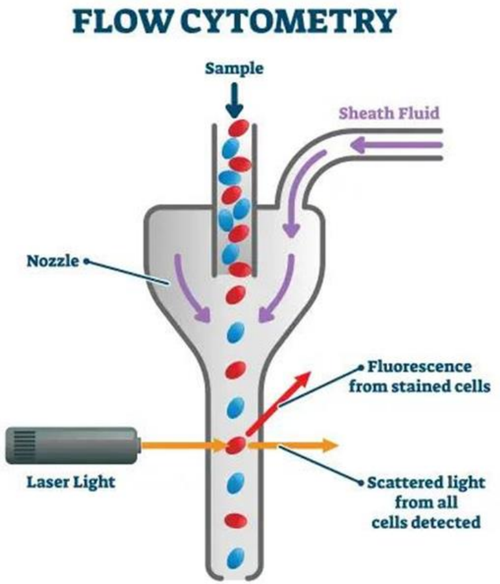

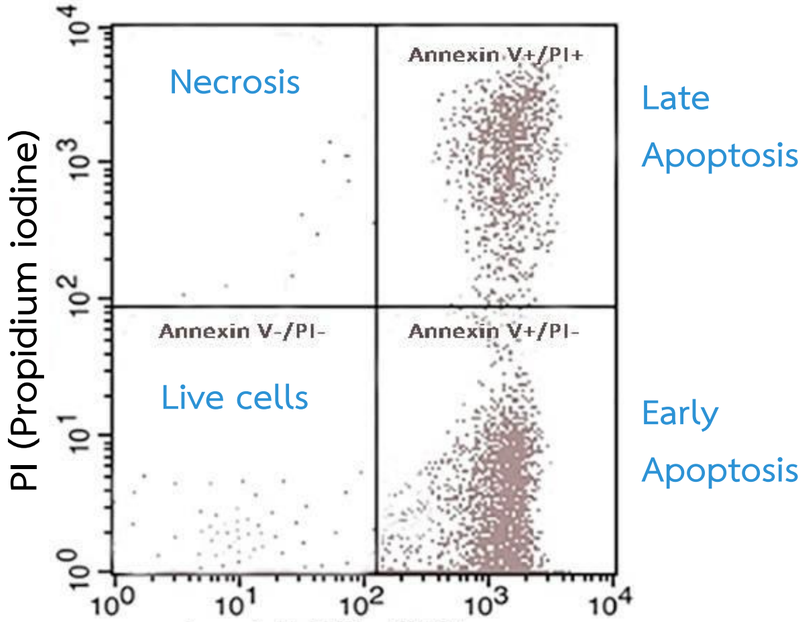

Annexin V-Alexa Fluor 488

≈10^6 MDA-MB-231 cells

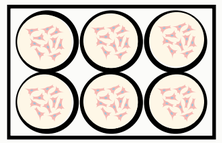

80% confluence

RAPTA-EA1 (10 µM)
or
Cisplatin (128 µM)

Incubated
at 37°C, 48 h., 5% CO_2

Washed twice with
PBS buffer

Centrifuged
300g, 5 min.

Collected
pellets

Resuspend cell pellets
in 100 µL of
1X Annexin-binding buffer

Added
Alexa-Fluor 488
Annexin-V
PI

Incubated
at RT

Added 1X
Annexin-binding
buffer

FACS canto flow cytometer

Results

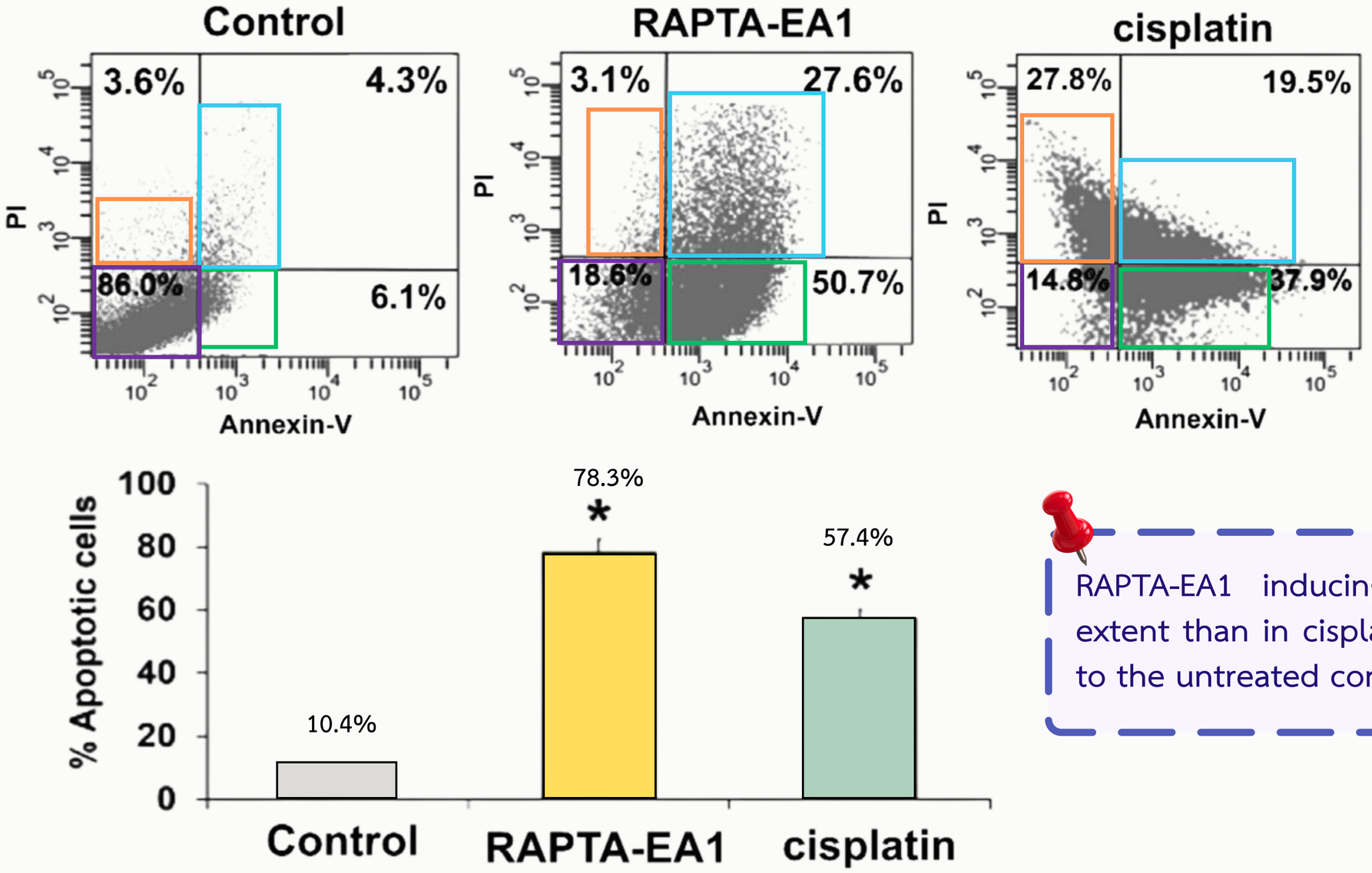

RAPTA-EA1 inducing apoptosis to a greater extent than in cisplatin-treated cells, compared to the untreated control cells.

Fig 3. Determination of starting apoptotic cells (Annexin V-positive/PI-negative) and late apoptosis cells (Annexin V-positive/PI-positive) following incubation with RAPTA-EA1 (10 μM) or cisplatin (128 μM) at 37 C for 48 h. Flow cytometric analysis was used to measure cells that bind Annexin V-Alexa Fluor 488 and PI apoptosis staining.

Immunofluorescence assay

Morphological change

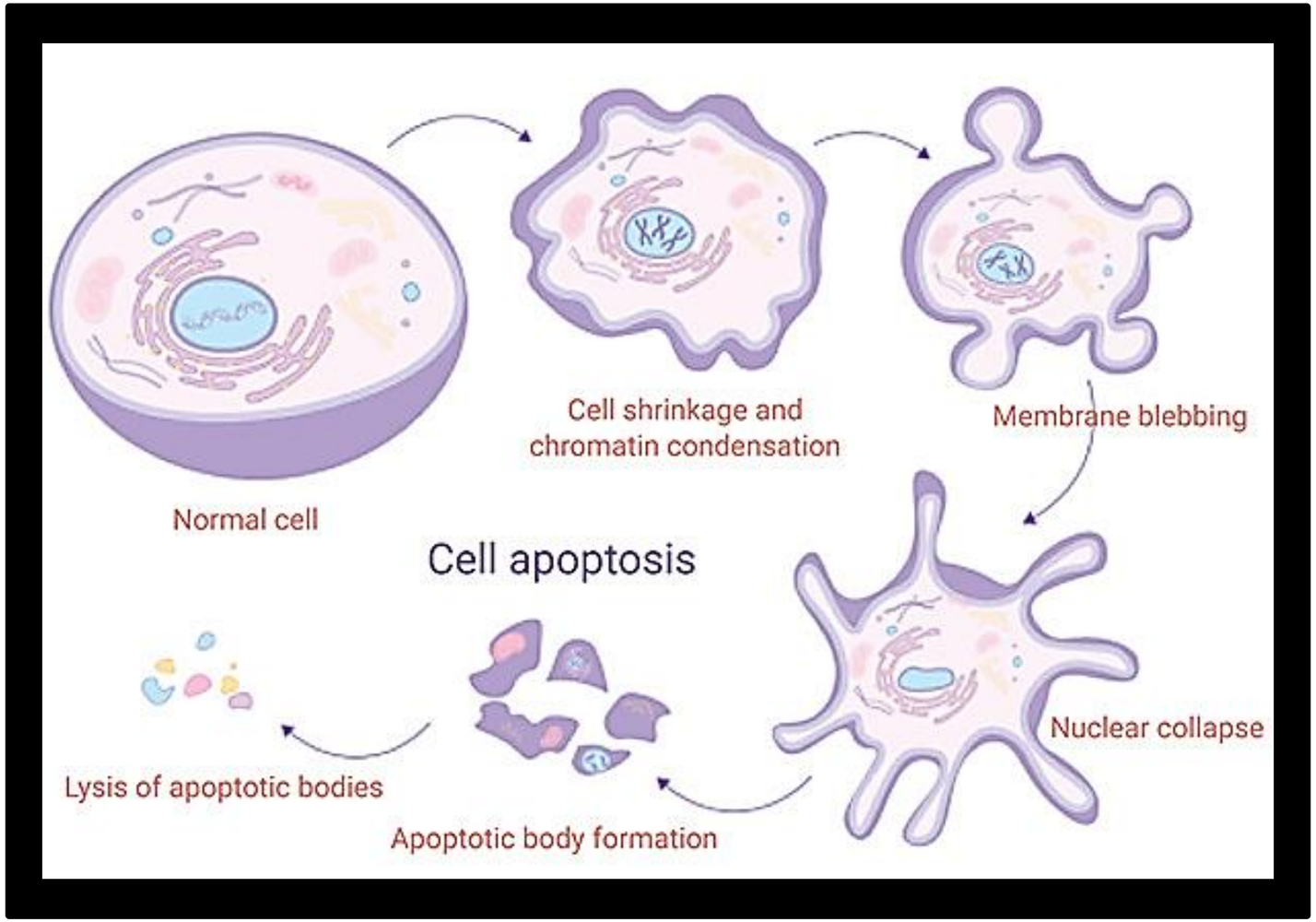

RAPTA-EA1 (10 µM)

MDA-MB-231 cells

Incubated
at 37°C, 48 h.

Fixed
4% paraformaldehyde

Permeabilized
0.2% Triton-x-100

Blocked with
3% BSA in 0.1% TBST

Incubated
RT, 1 h.

DAPI
4 µg/mL

Counterstained Nuclei

Detected by Fluorescence microscope

Results

Fig 4. Immunofluorescence assay. Cells treated with RAPTA-EA1 (10 μM) were seeded on coverslips, fixed using 4% paraformaldehyde for 30 min and then permeabilized using 0.2% Triton X-100. The cells were incubated with blocking reagent for 1 h at ambient temperature and then their nuclei were treated with counterstaining, 4',6-diamidio-2-phenylindole (DAPI; 1 μg/mL).

MDA-MB-231

Untreated | **RAPTA-EA1**

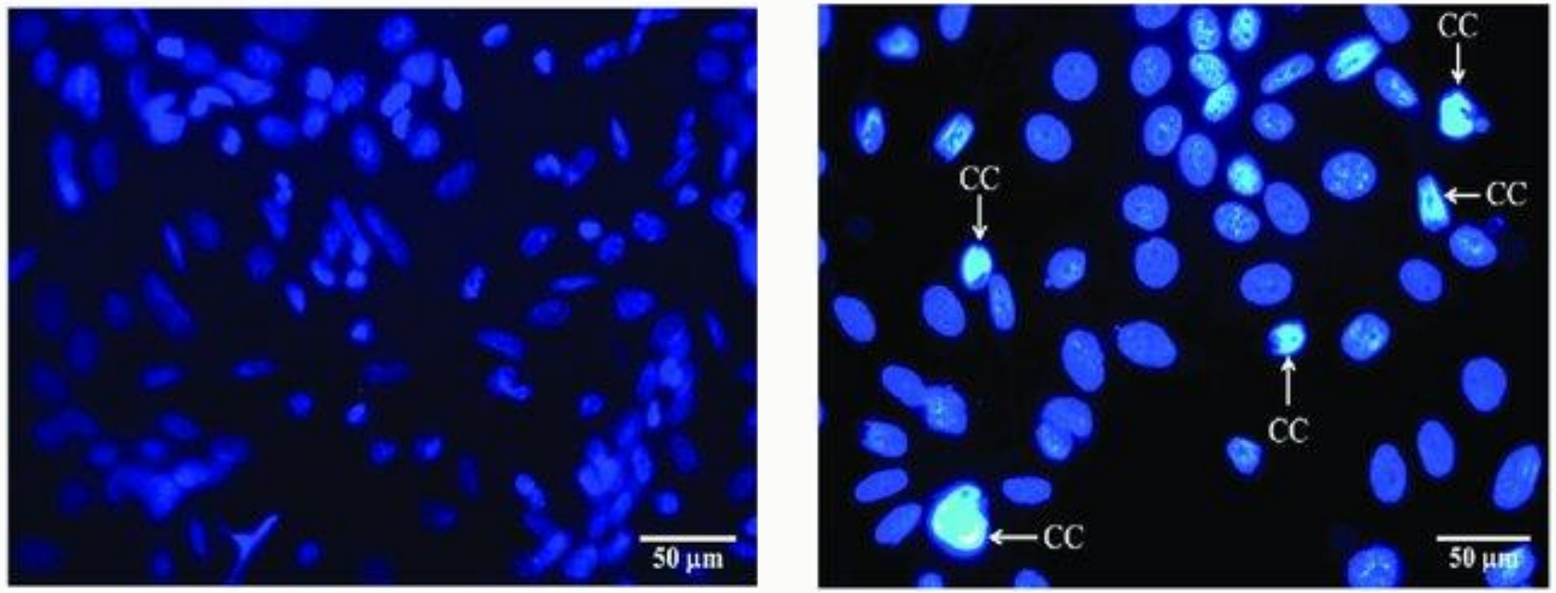

* CC = Chromatin condensation

RAPTA-EA1 induces a rippled nuclear contour and partial chromatin condensation, which are characteristics of nuclear condensation stage I in MDA-MB-231 cells, and is indicative of apoptosis.

Utilization of Quantitative PCR for cellular BRCA1 damage

BRCA1
(Breast cancer gene 1)

BRCA1 wild-type

MDA-MB-231

MCF-7

BRCA1-mutant

HCC1937

- BRCA1 have 5,936 - 11,986 bp
- BRCA1 involved DNA repair
- BRCA1 mutation → cell divide too much → Tumor or cancer

RAPTA-EA1 (0-100 μM)

MDA-MB-231 cells

Incubated

at 37°C, 48 h., 5% CO_2

Extracted genomic DNA
(BRCA1 exon11)

- Ruthenated genomic-DNA template 400 ng
- Forward & reverse primer 0.5 μM
- $MgCl_2$ cofactor 300 μM
- 1X Phusion GC buffer
- Phusion hot-start polymerase 2 units

Add PCR reaction mixture PCR The

PCR processing

Gel electrophoresis

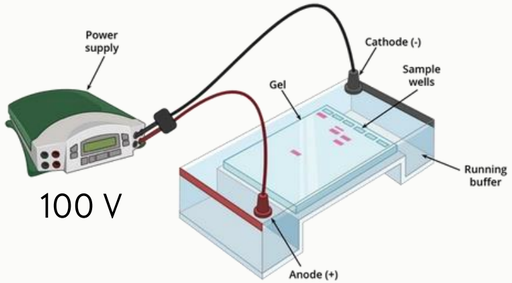

1% agarose gel

Ethidium bromide

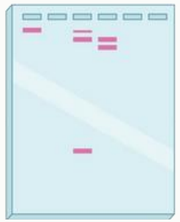

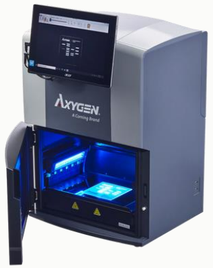

Visualized by UV light

Results

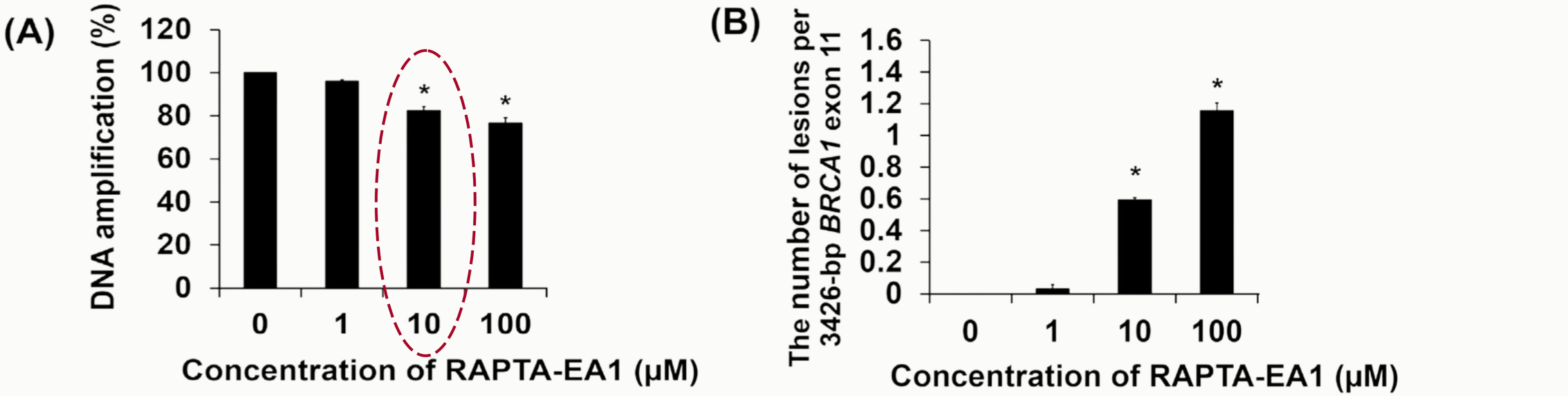

Fig 5. Cellular BRCA1 damage in MDA-MB-231 cells. Cells were incubated with RAPTA-EA1 at different concentrations (0-100 μM) at 37 C for 48 h. The fragment of BRCA1 was used as the DNA target which comprises 3426 bp located on BRCA1 exon 11. It was isolated from MDA-MB-231 cells, multiplied by PCR then the amplified DNA fragment was electrophoresed on 1% agarose gel. Staining was performed using ethidium bromide and imaged in the presence of ultraviolet light. The band intensity indicates the magnification of products quantified on a Bio-Rad Molecular Imager. The amount of DNA amplification (%) was plotted as a function of concentration (A). RAPTA-EA1-induced damaged BRCA1 fragment (lesions per the 3426-bp fragment) in MDA-MB-231 cells was calculated by the Poisson equation (B).

The growth of the BRCA1 gene decreasing as the RAPTA-EA1 concentration increases. The amplification of the BRCA1 gene decreased by 20% in the concentration range 10–100 μM, and DNA damage induce approximately lesion per BRCA1 fragment in the cells at 20% inhibition of DNA amplification.

Quantitative analysis of expression of BRCA1 mRNA following RAPTA-EA1 treatment using real-time quantitative RT-PCR

RAPTA-EA1 (10 μM)

MDA-MB-231 cells

Incubated at 37°C, 48 h.

Extracted

RNA

RNeasy® Mini Kit
(Qiagen, Germany)

Added reverse transcriptase

cDNA

QuantiTech®
Reverse transcription
(Qiagen, Germant)

Amplified

Added PCR components

SYBR green
Fluorescence dye

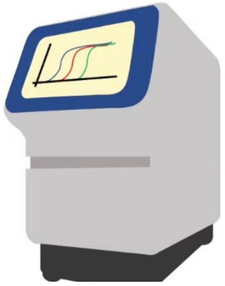

Real-time PCR machine

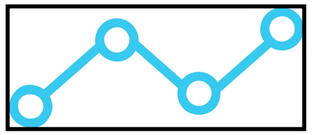

Analyzed data and normalized with β-actin

Specific primers

BRCA1 forward primer:
5′- GCCAGTTGGTTGATTTCCACC-3

BRCA1 reverse primer:
5′-GTCAAATGTGCTC CCCAAAAGC-3′

B-actin forward primer:
5′-CCGTAAAGACCTCTATGCCAACA3'

B-actin reverse primer:
5′-CGGACTCATCGTACTCCTGCT-3'

The Ct (cycle threshold)

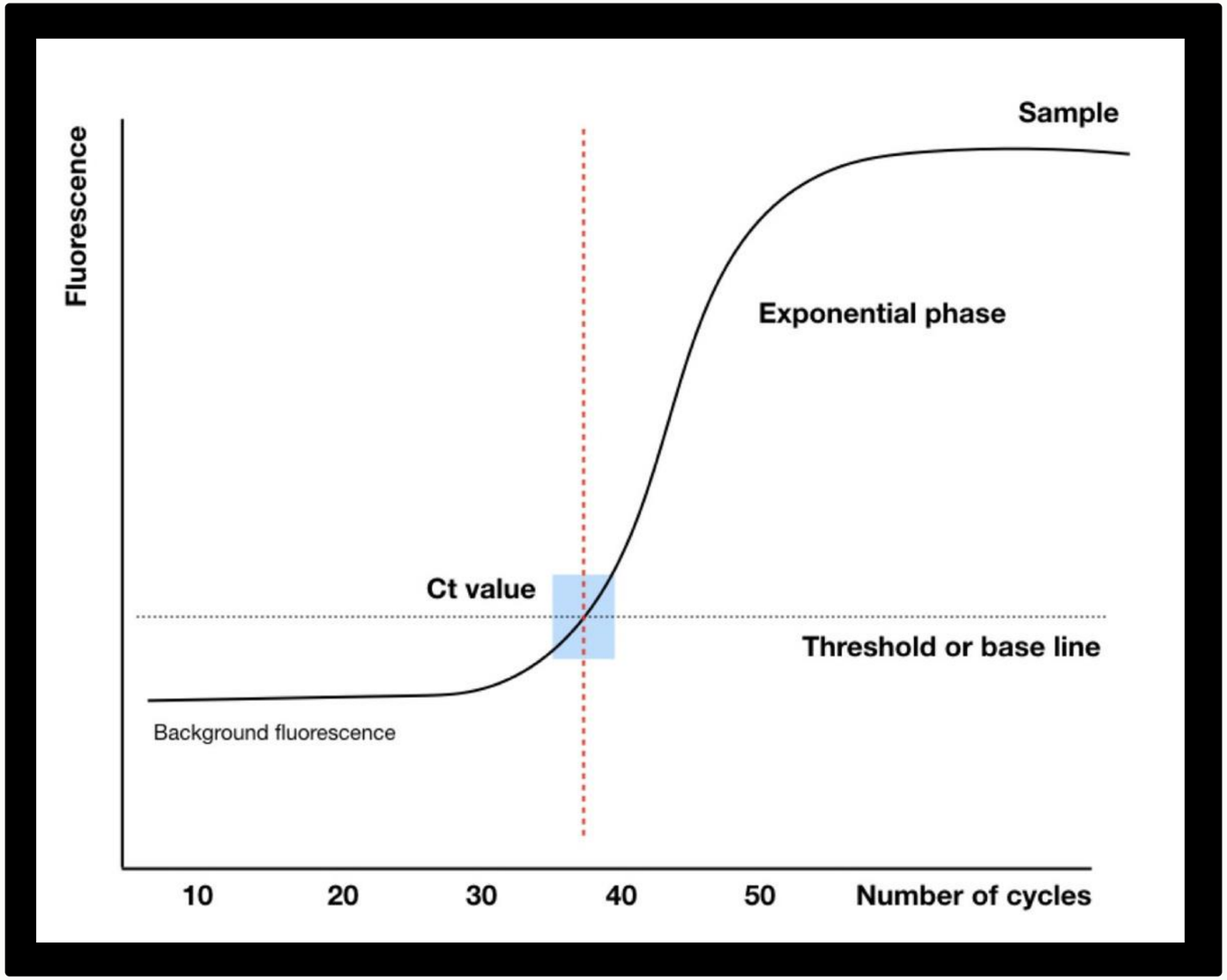

Definition:

- The number of cycles required for the fluorescent signal to cross the threshold (e.g., exceeds background level).
- Ct levels are inversely proportional to the amount of target nucleic acid in the sample.

Ct values ↓ **DNA/RNA ↑**

Results

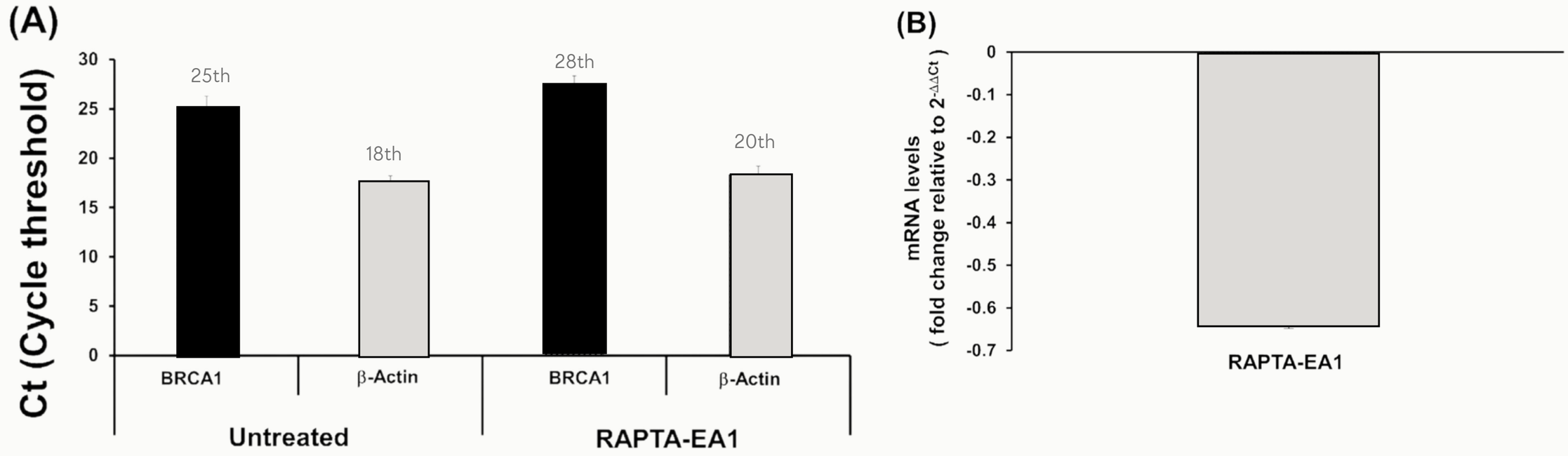

Fig 6. Effect of RAPTA-EA1 on the expression of BRCA1 mRNA and its protein in MDA-MB-231 cells. The transcribed BRCA1 gene was quantified by RT-PCR, normalized to the reference gene B-Actin and treatment-free control cells (A, B).

RAPTA-EA1 suppresses the expression of BRCA1 mRNA in MDA-MB-231 cells.

Western blot

RAPTA-EA1 (10 μM)

MDA-MB-231 cells

Incubated
at 37°C, 48 h.

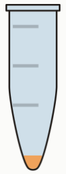

Collected cells

Lyzed cells

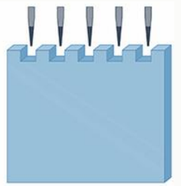

6% SDS-PAGE

SDS-Polyacrylamide gel electrophoresis

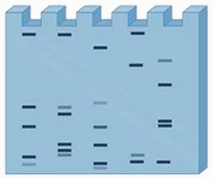

Separated Proteins

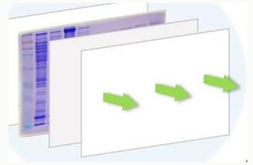

Transferred protein

Immunostained

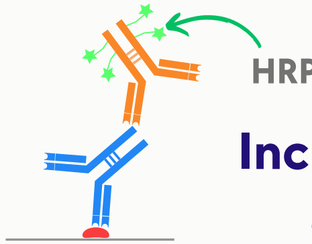

Incubated with antibody

Primary antibody;
Mouse monoclonal IgG1 antibody (BRCA1 (Ab1) Mouse (MS110)) at 1:1000 dilution

Secondary antibody;
Goat anti-mouse IgG conjugated with HRP at 1:5000 dilution

Gel imaging

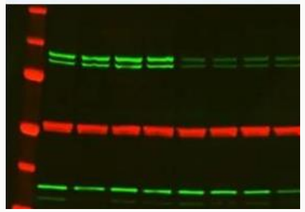

Visualized protein by chemiluminescence

Results

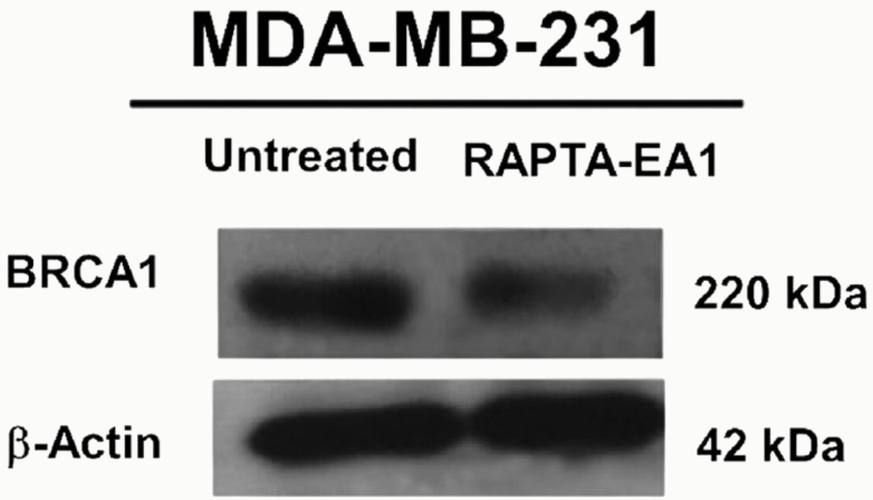

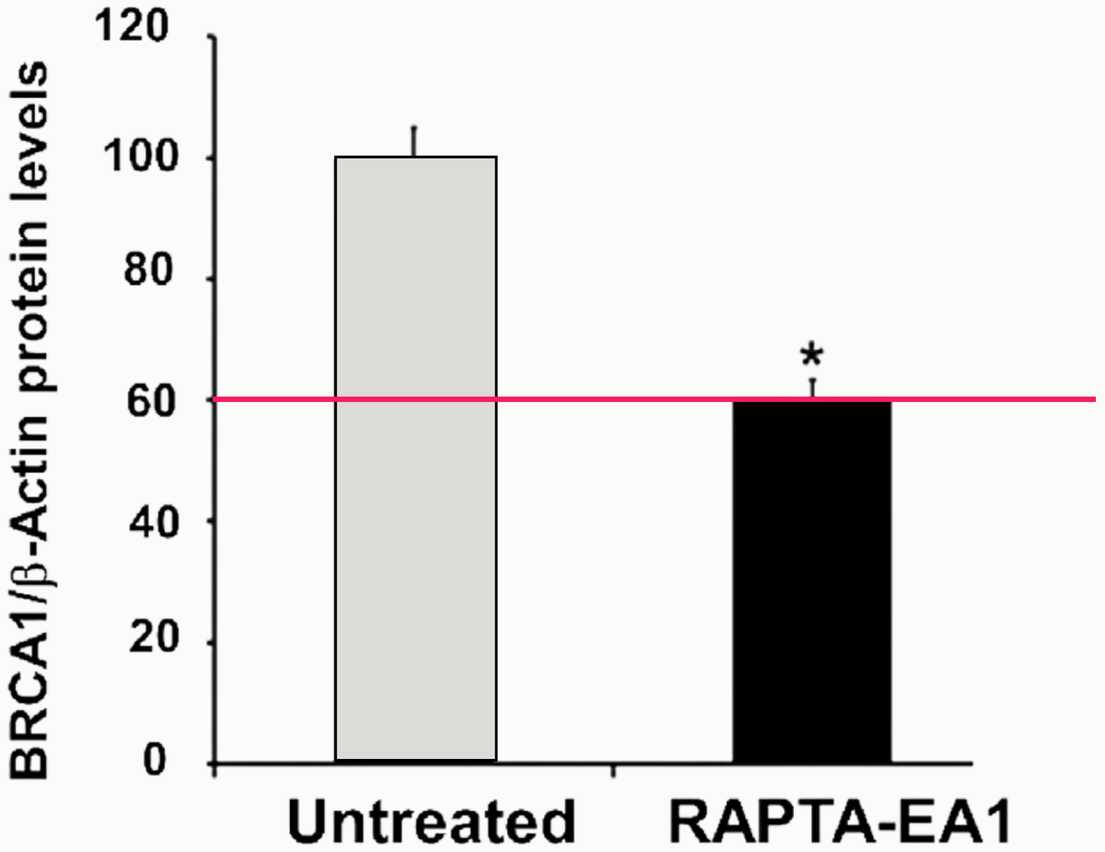

Fig 7. Protein expression was performed by Western blot analysis, normalized to the reference B-actin and treatment-free control.

Notably, BRCA1 protein expression was reduced by almost 50% compared to the untreated control cells.

Combination treatment

Objective:

- The combination treatment of RAPTA-EA1 and olaparib can reduce expression in BRCA1-wild type (MDA-MB-231 and MCF-7).

Methods:

- Cytotoxicity test (MTT assay)
- BRCA1 mRNA expression (RT-qPCR)
- BRCA1 protein expression (Western blotting)

MTT assay results

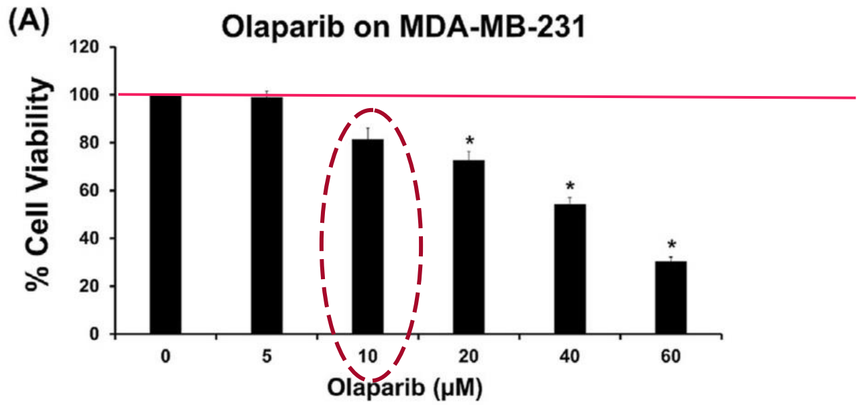

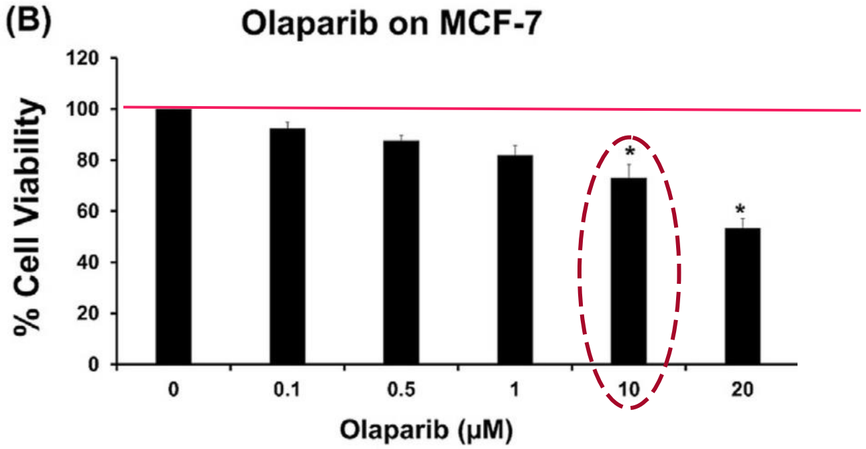

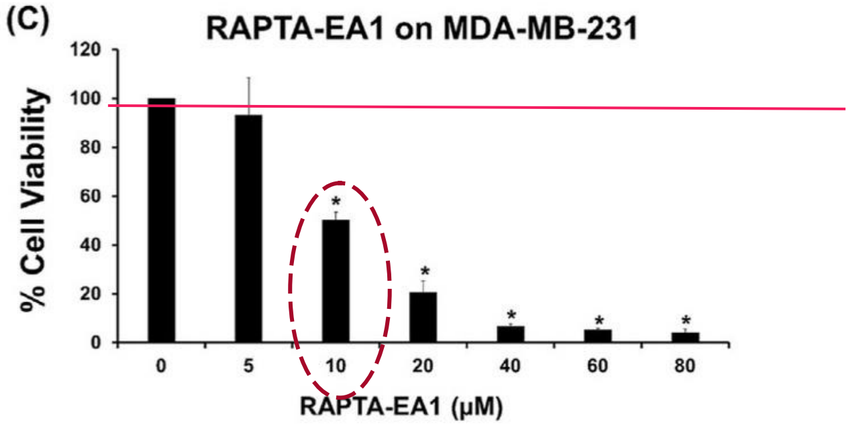

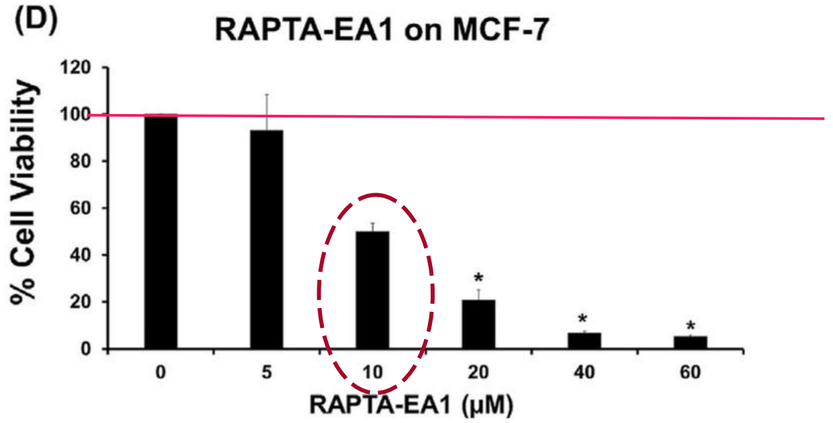

Fig 8. The cell growth inhibitory effect of olaparib alone and in combination with RAPTA-EA1. MDA-MB-231 and MCF-7 cells were treated with various concentrations of olaparib (A, B), RAPTA-EA1 (C, D) or olaparib in combination with RAPTA-EA1 (E, F) for 48 h at 37 C.

MDA-MB-231 cells are approximately 2-fold less susceptible to olaparib compared to MCF-7 cells, while RAPTA-EA1 is perfectly suppressed the viability of both cells at the same concentration.

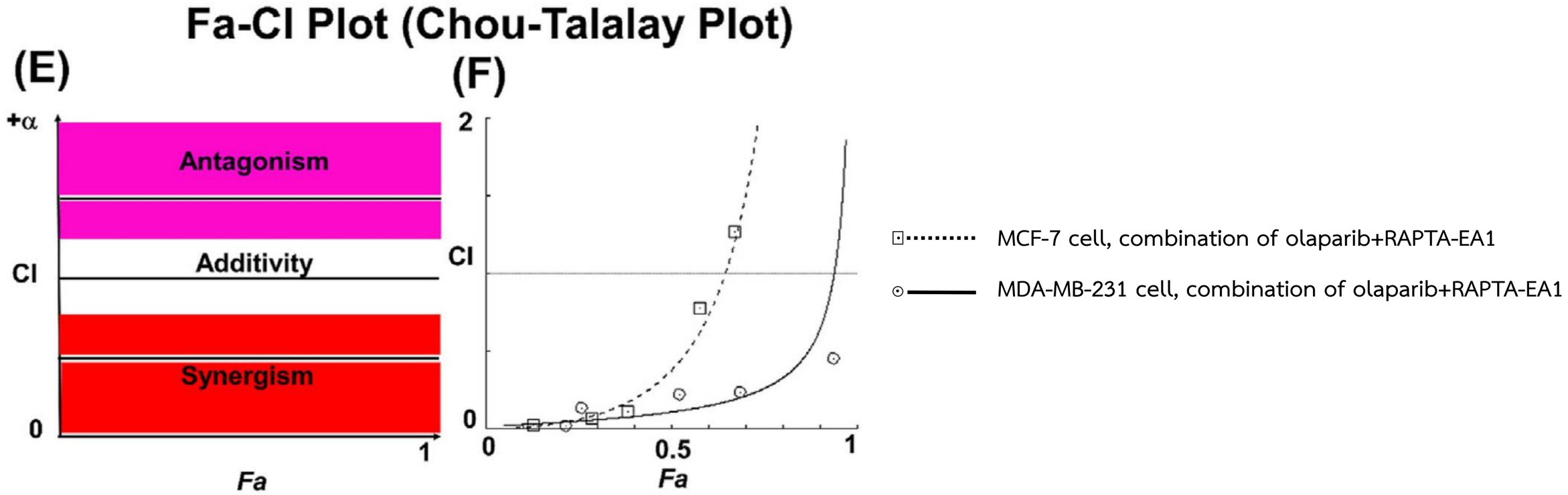

Fig 9. The cell growth inhibitory effect of olaparib alone and in combination with RAPTA-EA1. MDA-MB-231 and MCF-7 cells were treated with various concentrations of olaparib (A, B), RAPTA-EA1 (C, D) or olaparib in combination with RAPTA-EA1 (E, F) for 48 h at 37 C.

The combination of olaparib (10 μM) and RAPTA-EA1 (10 μM) results in a combination index (CI) of 0.24 (potent synergy) in MCF-7 cells and 0.78 (almost additive) in MDA-MB-231 cells.

RT-qPCR results

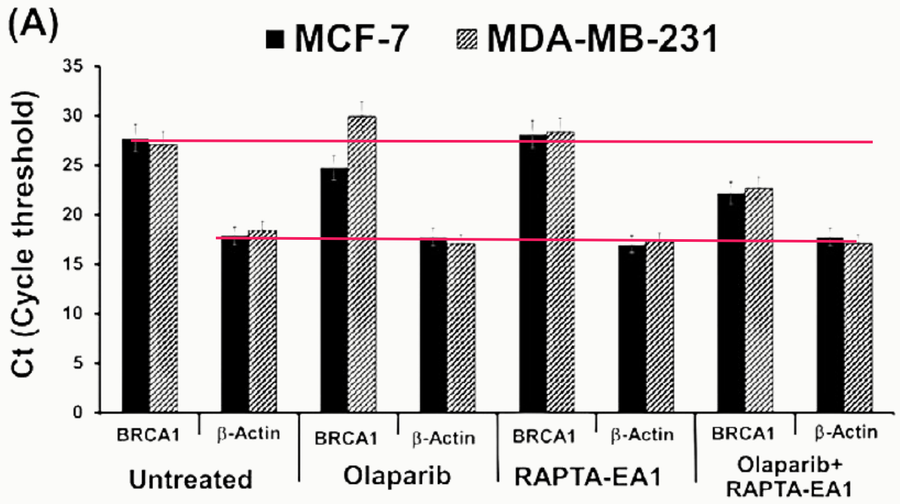

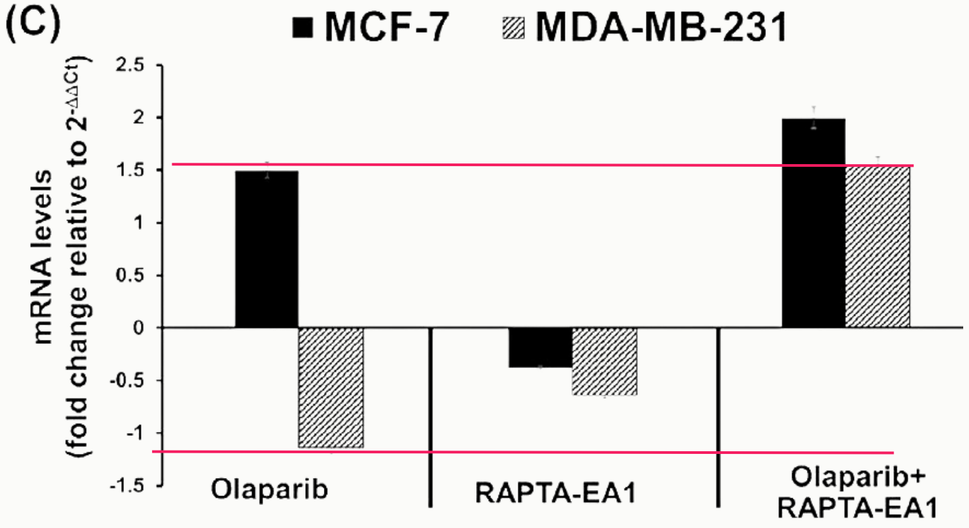

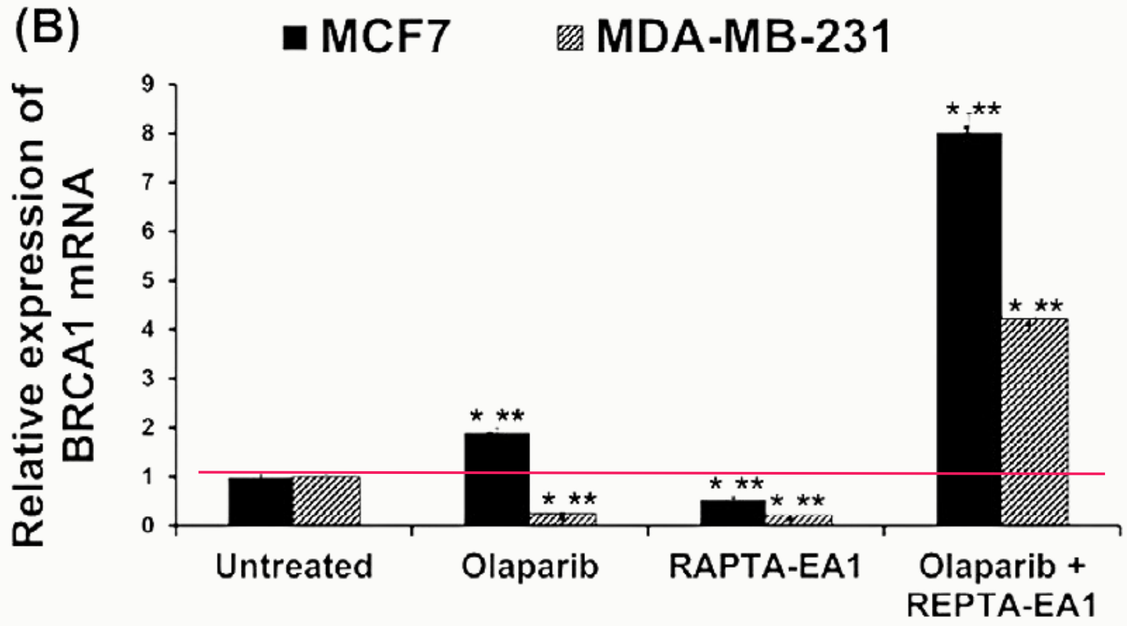

Olaparib downregulates the expression of BRCA1 mRNA in MDAMB-231 cells, whereas it is upregulated in MCF-7 cells. However, the combined inhibitors induce overexpression of BRCA1 mRNA in both cells (Figure A, B and C).

Fig 10. Differential expression of the BRCA1 mRNA and its protein. The amount of transcribed BRCA1 genes was determined quantitatively using RT-PCR, B-Actin expression was used as the normalized gene, compared to the untreated control cells. A: cycle threshold (Ct) for each sample, B: relative expression of BRCA1 mRNA, C: fold change for BRCA1 mRNA between MCF-7 and MDA-MB-231 sample.

Western blot results

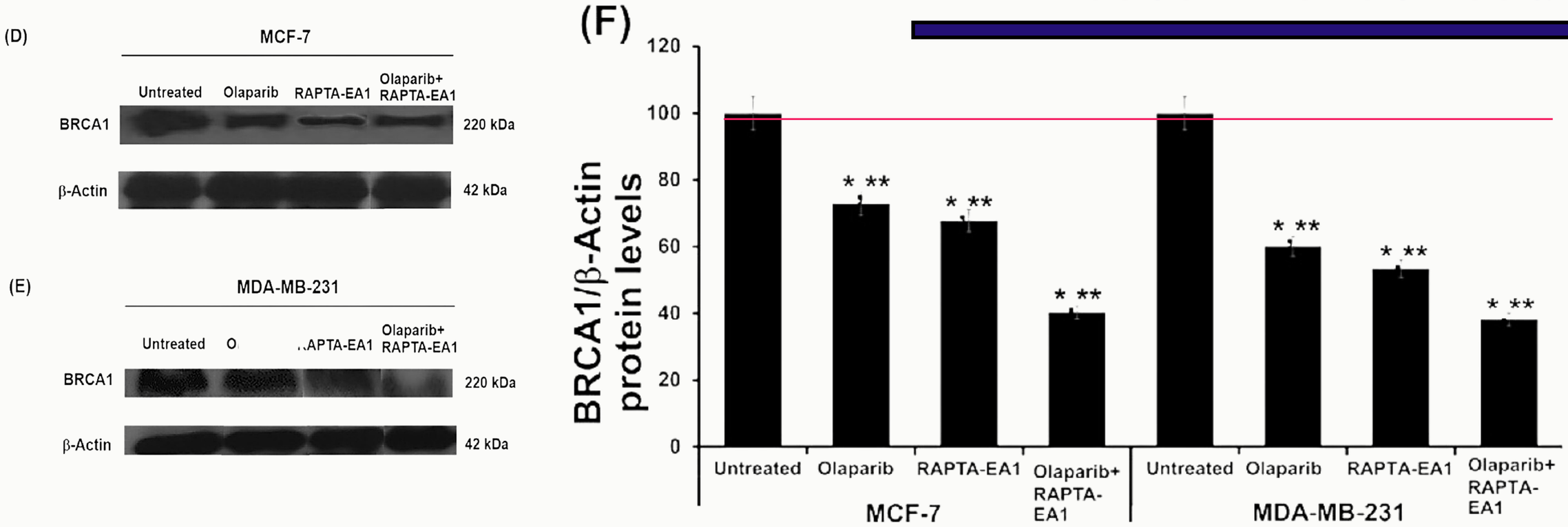

Fig 11. Differential expression of the BRCA1 mRNA and its protein. The amount of transcribed BRCA1 genes was determined quantitatively using RT-PCR, B-Actin expression was used as the normalized gene, compared to the untreated control cells. D-E (SI-Fig. 2), and F: Western-blot analysis of BRCA1 protein expression in cells treated with olaparib, RAPTA-EA1 and olaparib-RAPTA-EA1 combination.

The expression level of the BRCA1 protein is dramatically reduced after treatment with the olaparib-RAPTA-EA1 combination, compared with the untreated controls.

Conclusions

RAPTA-EA1 can inhibit MDA-MB-231 cells (TNBC cells) by cell cycle arrest and leading to apoptosis, decrease expression of BRCA1 mRNA and it's protein.

Combination treatment of olaparib-RAPTA-EA1 increased overexpression of BRCA1 mRNA, but expression of BRCA1 protein decreased in both cells.